

General Disclaimer

One or more of the Following Statements may affect this Document

- This document has been reproduced from the best copy furnished by the organizational source. It is being released in the interest of making available as much information as possible.
- This document may contain data, which exceeds the sheet parameters. It was furnished in this condition by the organizational source and is the best copy available.
- This document may contain tone-on-tone or color graphs, charts and/or pictures, which have been reproduced in black and white.
- This document is paginated as submitted by the original source.
- Portions of this document are not fully legible due to the historical nature of some of the material. However, it is the best reproduction available from the original submission.

(NASA-CR-168640) A LOW-POWER PHOTOVOLTAIC
SYSTEM WITH ENERGY STORAGE FOR RADIO
COMMUNICATIONS: DESCRIPTION AND DESIGN
METHODOLOGY (Jet Propulsion Lab.) 73 p
HC A04/MF A01

N82-19677

Unclas

CSSL 10B G3/44 J9287

A Low-Power Photovoltaic System With Energy Storage for Radio Communications

Description and Design Methodology

C. Phil Chapman
Jet Propulsion Laboratory

Paul D. Chapman
Everest and Jennings
Los Angeles, California

Alvin H. Lewison
Simpson Electric Company
Elgin, Illinois

January 15, 1982



Prepared for
U.S. Department of Energy
Through an Agreement with
National Aeronautics and Space Administration

by
Jet Propulsion Laboratory
California Institute of Technology
Pasadena, California

A Low-Power Photovoltaic System With Energy Storage for Radio Communications

Description and Design Methodology

C. Phil Chapman
Jet Propulsion Laboratory

Paul D. Chapman
Everest and Jennings
Los Angeles, California

Alvin H. Lewison
Simpson Electric Company
Elgin, Illinois

January 15, 1982

Prepared for
U.S. Department of Energy
Through an Agreement with
National Aeronautics and Space Administration
by
Jet Propulsion Laboratory
California Institute of Technology
Pasadena, California

Publication support for this report was provided by the Jet Propulsion Laboratory, California Institute of Technology, and the U.S. Department of Energy through an agreement with the National Aeronautics and Space Administration.

Publication of this report was sponsored by the United States Government. Neither the United States nor the United States Department of Energy, nor any of their employees, nor any of their contractors, subcontractors, or their employees, makes any warranty, express or implied, or assumes any legal liability or responsibility for the accuracy, completeness or usefulness of any information, apparatus, product or process disclosed, or represents that its use would not infringe privately owned rights.

Reference herein to any specific commercial product, process, or service by trade name, trademark, manufacturer, or otherwise, does not necessarily constitute or imply its endorsement, recommendation, or favoring by the United States Government or any agency thereof. The views and opinions of authors expressed herein do not necessarily state or reflect those of the United States Government or any agency thereof.

ABSTRACT

A low-power photovoltaic system was constructed with approximately 500 amp-hours of battery energy storage to provide power to an emergency amateur radio communications center. The system can power the communications center for about 72 hours of continuous no-sun operation. Complete construction details and a design methodology algorithm are given with abundant engineering data and adequate theory to allow similar systems to be constructed, scaled up or down, with minimum design effort.

ACKNOWLEDGMENT

I would like to thank my son, Paul D. Chapman, for designing and building the array framework and battery box and for writing that portion of the report describing the construction details of those elements of the system.

I would also like to thank Alvin H. Lewison for specifying the analog meter requirements, designing the meter panel, and writing that part of the report describing the system metering. He was also responsible for testing the array amp-hour meter and determining its accuracy.

Ronald S. Slusser designed the meter panel silk screen and built the necessary contrivance to allow us to successfully silk screen the panel on the third try, using the facilities of Pasadena City College.

Special thanks are in order for the vendors and manufacturers who donated components for the system.

And, finally, I appreciate the technical review of this report by Gerald Prayer and Ronald Ross. Their suggestions were quite helpful in ensuring the technical integrity of this report.

Publication of this report was provided by the Jet Propulsion Laboratory under Task RD-152, Amendment 200, which is sponsored by the U.S. Department of Energy under Interagency Agreement DE-AI01-76ET20356 with NASA.

CONTENTS

I.	INTRODUCTION	1-1
	A. PURPOSE	1-1
	B. SYSTEM FUNCTION	1-1
II.	APPROACH	2-1
III.	IMPLEMENTATION	3-1
	A. BASIC SYSTEM CONCEPTS	3-1
	B. PHOTOVOLTAICS	3-1
	1. Mechanical	3-1
	2. Electrical	3-6
	C. ENERGY STORAGE AND REGULATION	3-11
	1. Mechanical	3-11
	2. Electrical--General	3-14
	3. Shunt Regulator	3-18
	4. Battery Pack	3-21
	5. Battery Power Dissipation	3-25
	D. POWER CONVERSION	3-26
	1. AC Inverter	3-26
	2. DC Converter	3-26
	E. METERING	3-27
IV.	ENERGY STORAGE SYSTEM DESIGN	4-1
	A. STATION SYSTEM DESCRIPTION	4-1
	B. BATTERY STORAGE DESIGN METHODOLOGY	4-1
	C. CONSIDERATIONS FOR SPECIFYING RECHARGE TIME	4-10

V.	ENERGY DISTRIBUTION SYSTEM	5-1
A.	GROUNDING SYSTEM	5-1
B.	VOLTAGE DROPS	5-2
C.	RADIO ROOM CONTROL	5-2
D.	SAFETY	5-4
VI.	SUMMARY, PHILOSOPHY, AND RECOMMENDATIONS	6-1
	REFERENCES	7-1

APPENDIX

	PROCEDURES FOR CALCULATING THE AVERAGE TRANSMITTANCE OF SOLAR ENERGY THROUGH THE EARTH'S ATMOSPHERE	A-1
--	---	-----

Figures

1.	PV System: (a) Simple Representation; (b) Advanced Representation	3-2
2.	Sensor Technology Module Photograph: (a) Front; (b) Back	3-3
3.	Sensor Technology Module Drawing	3-4
4.	PV Array Framework	3-5
5.	I-V Module Characteristics	3-8
6.	Schematic Diagram of a PV Array Configuration	3-8
7.	Protective Diode Applications: (a) Shorted Cells, No Protective Diodes; (b) Shorted Cells, Protective Cells; (c) Shadowed Cells, No Protective Diodes; (d) Shadowed Cells, Protective Diodes	3-9
8.	V-I Characteristics of Low-Current Schottky Diodes	3-10
9.	Battery Box Floorboard	3-12
10.	Battery Modules on the Floorboard	3-13
11.	Battery Box	3-15

Figures (Cont'd)

12.	Battery Box Bus Bar Configuration	3-16
13.	Schematic Diagram of an Advanced Conceptual PV System	3-17
14.	V-I Characteristics of the Schottky Isolation Diodes	3-17
15.	Schematic Diagram of a System Shunt Regulator	3-18
16.	DC Gain Versus Collector Current, TRW SVT 6062 Darlington	3-19
17.	Shunt Impedance as a Function of Array Current and Float Voltage	3-20
18.	Battery Module Configuration	3-22
19.	Relationships Among Float Voltage, Open-Circuit Voltage, and Thermal-Neutral Voltage	3-25
20.	System Meter Panel	3-29
21.	Meter Wiring Schematic Diagram	3-30
22.	Array Amp-Hour Meter Schematic Diagram	3-31
23.	Station Communication Equipment	4-2
24.	Bus Bars and Regulator Heat Sinks	4-3
25.	Batteries, Regulator Box, and Inverter Relay	4-4
26.	Batteries, Inverter, and Breaker Switch Box	4-5
27.	Breaker Panel	4-6
28.	PV Array	4-7
29.	Battery Sizing Methodology	4-8
30.	Temperature Effects on Cell Performance	4-12
31.	PV System Accumulative Amp-Hours Function	4-13
32.	PV System Array Current Function	4-14
33.	High-Sun Nominal System Voltages and Currents	5-1
34.	AC Control and Distribution Schematic Diagram	5-3
35.	Radio Room Metering and Control Schematic Diagram	5-3
36.	PV System Circuit Breakers	5-5

Tables

1.	Communications Equipment Current and Power Requirements	2-1
2.	Standard Operating Characteristics, PV System Module	3-7
3.	PN Junction Versus Schottky Diode Trade-Off	3-10
4.	Prediction of Battery Pack Performance: 50/50 Duty Cycle . . .	3-23
5.	Prediction of Battery Pack Performance: 30/70 Duty Cycle . . .	3-24
6.	Prediction of Battery Pack Performance: 10/90 Duty Cycle . . .	3-24
7.	Meter Panel Complement	3-28
8.	Daily Array Output Versus Peak Ambient Air Temperature	4-11
9.	Atmosphere Model Beam Radiation Prediction	4-12
10.	Station Steady-State Current Overhead (Accumulative)	5-4
A-1.	Summary of Solar Ephemeris	A-3

SECTION I

INTRODUCTION

A. PURPOSE

The purpose of this report is to describe in detail the design and construction of a small photovoltaic (PV) system that has all of the elements of larger systems. Using the design concepts and techniques described herein will allow similar systems to be assembled--scaled up or down in peak power and energy storage. What follows is not the only design approach. It is, however, a description of a system approach that provides a methodology for the design and construction of PV systems with requirements for energy storage, power conditioning, and power distribution management.

B. SYSTEM FUNCTION

Two-thirds of the State of California is vulnerable to a great quake. Seismologists indicate a much-better-than-chance probability that a great quake could occur in Southern California any time in the next several years. In such an event, commercial and emergency service communications will be disrupted over a widespread area. The extent and consequences of this disruption will be determined by the proximity of the quake epicenter to the metropolitan areas.

The communication requirements during such a disaster will be determined by the extent of the structural damage and resulting population mortality. For example, a great quake centered along the San Andreas fault immediately northeast of Los Angeles can be expected to create widespread damage from Santa Barbara to the north through San Diego to the south.

An amateur radio-based emergency communication center has been assembled to help provide temporary communications immediately following a catastrophic disaster such as a great quake centered near Los Angeles. The radio equipment operates from storage batteries receiving energy from the sun and is not dependent upon utility-delivered electrical energy.

Sunlight is converted to electrical energy by means of photovoltaic (PV) modules composed of silicon solar cells. These modules were obtained from the U.S. Department of Energy through the Jet Propulsion Laboratory (JPL) Lead Center for Photovoltaic Technology Development and Applications. The modules are used to supply electrical energy to the communications equipment.

The amateur radio station is situated in a favorable location 610 m (2,000 ft) above sea level north of Los Angeles. From this location it is possible to have high-frequency (144 MHz), two-way communications from Santa Barbara 160 km (100 mi) to the north, the metropolitan areas of Ventura, Los Angeles, and Orange Counties, and San Diego 233 km (145 mi) to the south--a total population of over 13 million. In addition, lower frequency (3.5 to 29 MHz) communications can be conducted simultaneously, if necessary, with other amateur radio stations

outside the high-frequency range. This includes the remainder of the state and, at least, all the other states. These communications can be accomplished using radio-frequency power levels of less than 200-W input. This is possible because of the favorable station location.

SECTION 11

APPROACH

Sizing a PV array and energy storage system for emergency communications equipment is a difficult task, which is unique to the application. One has to resolve such questions as:

- (1) How long do emergencies last?
- (2) What is the expected duty cycle (i.e., the ratio of transmit-to-receive)?
- (3) How much time is there between emergencies?
- (4) How long should it take to recharge the battery pack after a drill or emergency?
- (5) How much storage capacity is required?

Except for the last question, these questions are not encountered in most PV systems applications. Attempting to answer the above questions forced a systems design approach which is described in this report.

In general, PV modules for any application have to be connected in parallel and, perhaps, in series and parallel to meet the voltage and current requirements of the equipment. Then the modules must be fastened into a framework that can be tilted at a favorable angle to the sun. The current-voltage characteristics of any PV array will be influenced by the battery storage requirements along with the equipment power requirements. It is necessary to look at the entire system requirements before starting the design and construction. In addition, a decision has to be made as to the desired lifetime of the system, and provisions must be made for component and equipment expansion over the design lifetime.

Table 1 lists the current and power requirements for this system's high- and low-band communications equipment. Worst-case conditions occur when both radios are in the transmit mode at the same time. This would draw 24 A (at a

Table 1. Communications Equipment Current and Power Requirements

FREQUENCY BAND	RECEIVE MODE		TRANSMIT MODE	
	amps	POWER, W	amps	POWER, W
HIGH	0.20	2.72	9.10	124
LOW	6.00	81.6	15.0	204
BOTH	6.20	84.3	24.1	328

design voltage of 13.6 V) from the battery pack. There could be additional battery current drain from the DC-to-AC inverter (used for antenna rotation motors) and from emergency lighting in the radio room.

The information in Table 1 was easy to obtain from the equipment manufacturers' operation manuals. But duty cycles (ratio of transmit-to-receive time) had to be defined to size the battery pack. It was determined that some manufacturers of emergency service communications equipment (i.e., police, ambulance, and fire department service) design for an expected average duty cycle of 10 percent transmit, 10 percent receive, and 80 percent standby. Standby here is defined as ready to receive, i.e., squelch mode. Based upon this information, the following duty cycles were defined:

- (1) Critical emergency traffic
 - (a) 10 percent transmit
 - (b) 90 percent receive
- (2) Noncritical traffic
 - (a) 30 percent transmit
 - (b) 70 percent receive
- (3) Rag-chew (station-to-station, non-net)
 - (a) 50 percent transmit
 - (b) 50 percent receive

The low-band equipment does not have squelch control, so the squelch mode and receive mode are the same. In addition, this mode includes filaments in the final amplifier tubes. The high-frequency equipment does have a squelch mode but the receive mode, as can be seen from Table 1, is such a small current drain that the receive and squelch modes are also lumped together. In addition, the transmit mode for the high band includes a 40-W linear amplifier which may or may not be required.

The battery pack was to consist of an unknown number of improved electric-car, deep discharge 6-V lead-acid modules. Extensive modeling and laboratory tests and verification of models had previously been performed on these types of batteries through Department of Energy funding. Since mathematical expressions were known for these batteries relating amp-hour capacity as a function of discharge current and electrolyte temperature, and relating specific power (density) as a function of specific energy (density), it was possible to predict battery pack performance as a function of the data presented in Table 1 and electrolyte temperature. A worst-case battery complement would assume no output from the PV array but batteries fully charged. By argument and arbitration, it was decided to design for 72 hours of continuous operation in total darkness, using the critical emergency traffic duty cycle.

Based upon the approach described above, and the methodology defined in this report, 24 Sensor Technology (Photowatt) model 20-10-1674 (block III) PV modules were transferred from the Department of Energy to the design team through the JPL lead center. The lead center had the responsibility of reviewing and modifying the preliminary design prior to the transfer and is responsible for site inspection periodically to be assured that the PV modules are used as intended.

Of the 24 modules obtained, 22 are used as the PV array and 2 are kept as spares. The system design is based on a 10-year lifetime.

SECTION III IMPLEMENTATION

A. BASIC SYSTEM CONCEPTS

The photovoltaic modules supply power to the communications equipment. During no-sun periods, batteries are used to supply the power. During sun periods when only some or no power is required from the system, the PV energy is stored in these batteries. Figure 1(a) illustrates the simplest system concept. The blocking diode prevents the battery pack from discharging back through the PV array during no-sun periods. The problem with this simple concept is that all the electrolyte would boil away in the batteries when the batteries became fully charged and the equipment was off. A more advanced concept of the system is seen in Figure 1(b). Here a shunt regulator is used to maintain the battery pack voltage independent of the state of charge of the battery pack (R_S) or the load. When the battery pack is fully charged and the equipment is not operating, the PV array energy is dissipated as heat in the shunt regulator, and the system efficiency is at its worst. If the battery pack is partially discharged, if the equipment is operating, or if both conditions exist, the PV array current will be allocated to meeting the load requirements, and any surplus current will be used to recharge the battery pack with no current being dissipated in the shunt regulator. During the time and conditions that the PV array energy is required, the system operates at its highest efficiency.

The dynamic resistance of the array, regulator, battery, and the load (Figure 1b) and the associated time constants of the loop (the system) are important parameters and will affect the system stability.

B. PHOTOVOLTAICS

1. Mechanical

Figures 2(a) and 2(b) are photographs of the front and rear of the Sensor Technology PV module, and Figure 3 is a drawing of the module with detailed dimensions (used by permission from Reference 1).

Each of the 22 modules used to supply energy to the system measures approximately 58 by 28 cm (28 by 11 in.) and is 4.6 cm (1.8 in.) in depth and weighs 3.7 kg (8.2 lb). Each module is constructed within an aluminum heat sink, as shown in Figure 2(b). The silicon cells (44 per module) absorb heat from the sun, and the heat derates their performance. The heat sink provides a means of dissipating this heat. If a module is set on a nonconducting surface on a warm sunny day, it gets so hot that it can't be handled with bare hands! Therefore, the modules were mounted in an aluminum framework that allows heat to be transferred away from the heat sink by convection and radiation. Care was taken not to mount the PV array too close to the shake roof surface, which itself transfers heat by convection and radiation.

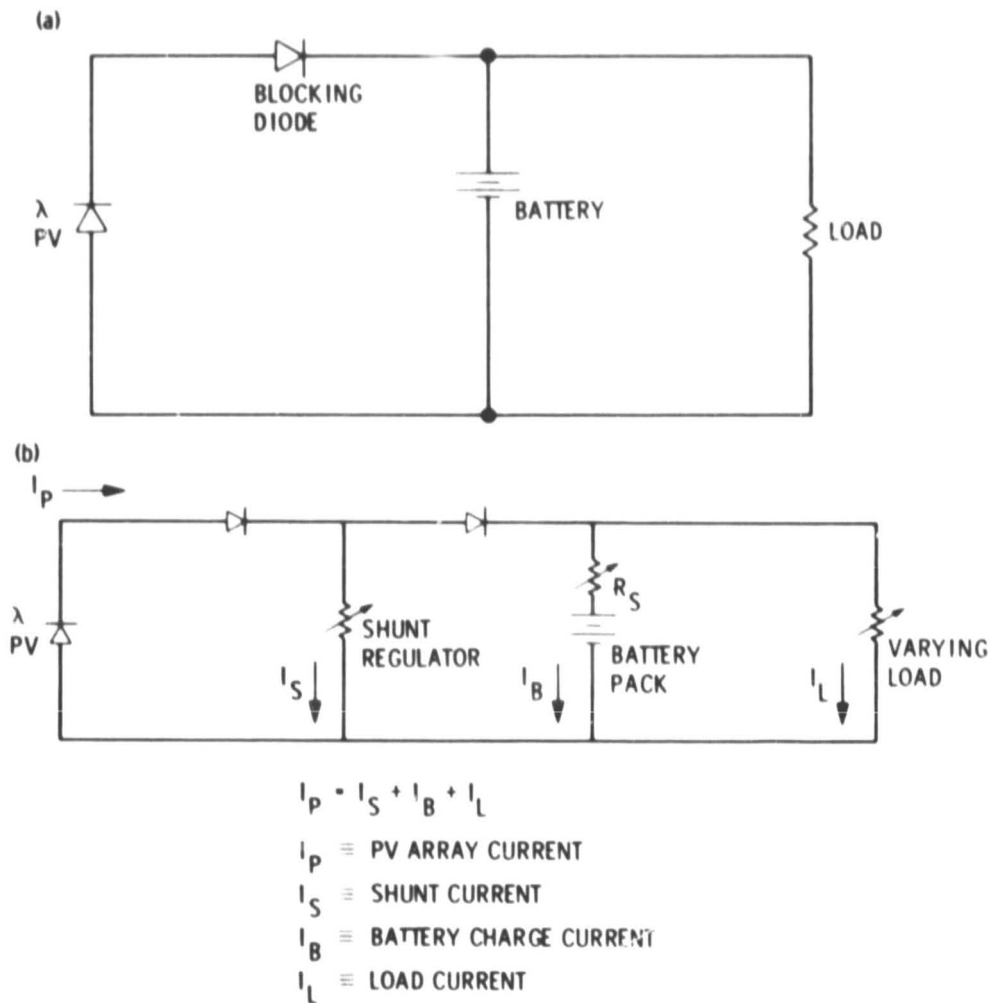


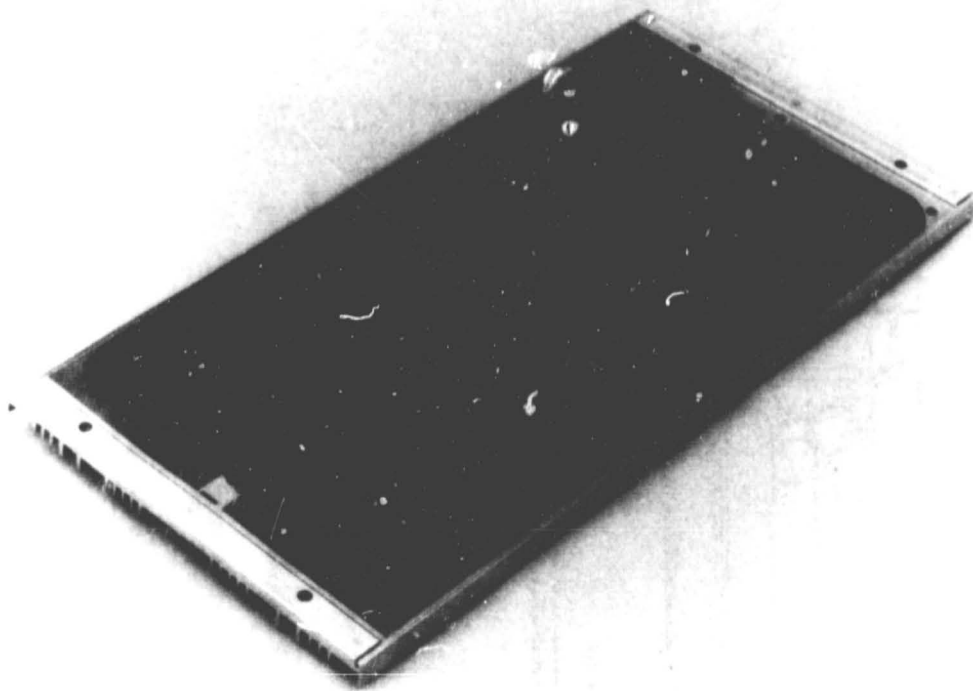
Figure 1. PV System: (a) Simple Representation; (b) Advanced Representation

Strength, rigidity, weight, and zero maintenance were the primary considerations in designing the module structure. 6061 aluminum (6063 for extruded shapes) was selected as the primary material to be used in the construction. This was based on cost, weight, and availability.

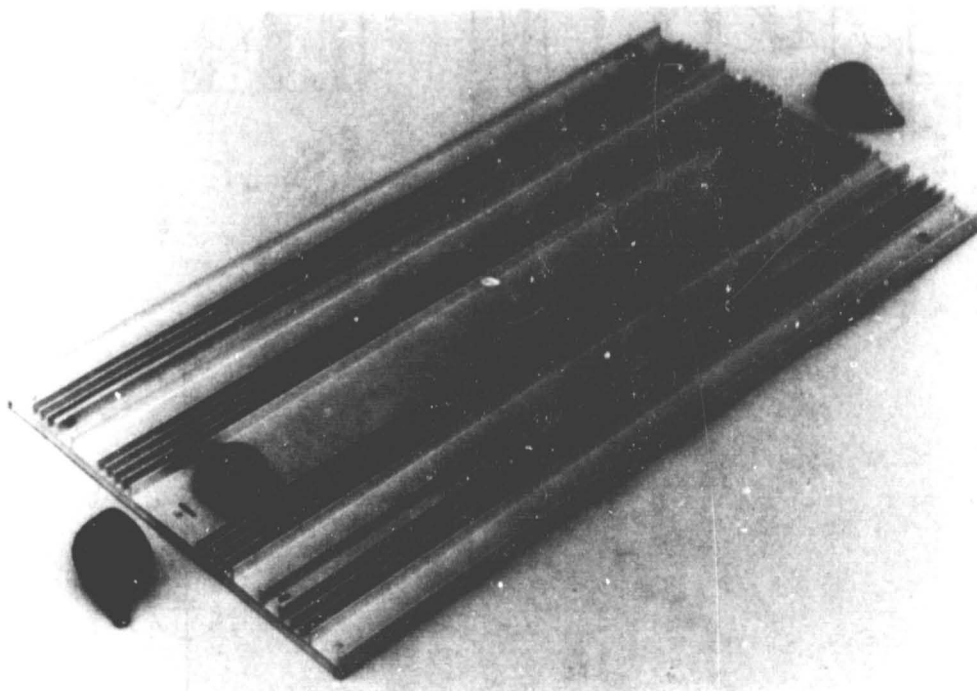
Figure 4 shows the assembled array. The structure measures 326 cm (129 in.) long and 119 cm (47 in.) wide, with a 326-cm extended tee section running lengthwise through the middle. This provides adequate space for two rows of eleven modules to be mounted on the structure with about 1 cm (0.38 in.) between modules.

The structure is constructed entirely of 1 1/2- by 1 1/2- by 1/8-in. aluminum angle, except for the center tee section which is 2- by 3/4- by 1/8-in. The center of the structure is braced with two 119-cm (47-in.) sections of angle as

ORIGINAL PAGE
BLACK AND WHITE PHOTOGRAPH



(a)



(b)

Figure 2. Sensor Technology Module Photograph: (a) Front; (b) Back

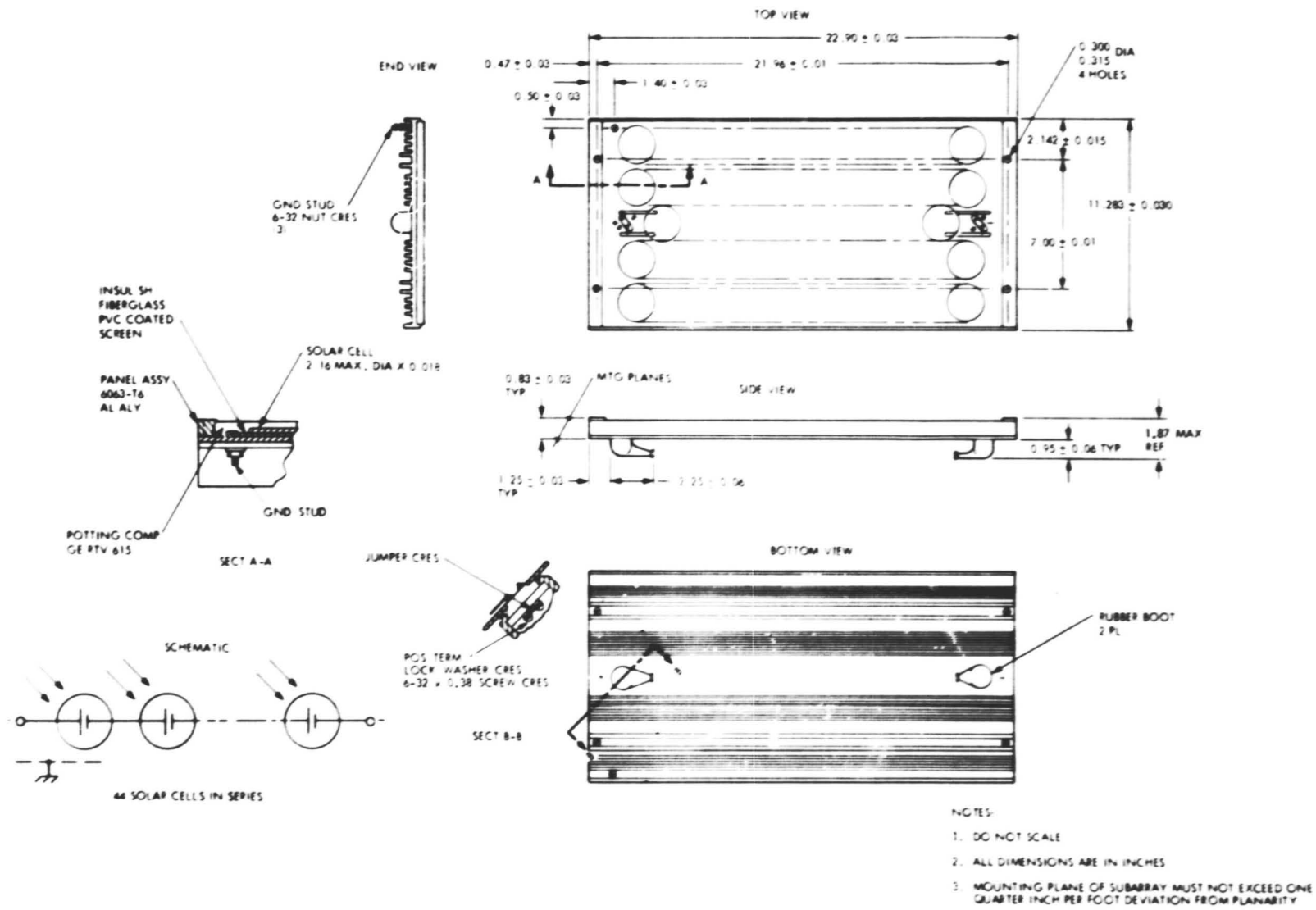


Figure 3. Sensor Technology Module Drawing

ORIGINAL PAGE
BLACK AND WHITE PHOTOGRAPH



3-5

Figure 4. PV Array Framework

seen in Figure 4. End areas and center areas are braced with 1/4-in. aluminum bar stock, which provides extra rigidity at section interfaces.

The array structure rests on six legs made of 1- by 1- by 1/8-in. extruded rectangular aluminum tubing. Inside this tubing is 3/4- by 3/4- by 1/8-in. rectangular tubing. These legs, in turn, are set inside 8- by 1 1/8- by 3/16-in. channel sections. The entire assembly is butted up against 4- by 4- by 1/4-in. 90° angle brackets.

The angle brackets are fastened with 3/8- by 1 1/2-in. lag bolts to 2- by 4-in. cedar studs, which were mounted with 12-in. bolts through the shake roof to the ceiling rafters below.

Unfortunately, nothing was co-planar since a wall angle (array azimuth angle)¹ of zero degrees (i.e., geographic south) was desired and the roof was off south by a few degrees. Therefore, this type of design provided the greatest degree of flexibility when positioning the platform on the roof at the desired tilt and wall angles.

After the array structure was in the desired position, residual rectangular tube and angle material was used to diagonally brace the legs to help insure strength and rigidity. Fifty-mile-an-hour wind gusts are not uncommon during the windy season, so guy cables were used to additionally fasten the array structure to the cedar studs. Clearance was provided to prevent air compression under the structure and allow the prevailing (normal) breezes to convectively cool the PV module heat sinks.

The array structure fasteners were 3/8 in.-16 by 1-in. hex head bolts and the modules were attached to the platform with 1/4 in.-20 by 1 1/2-in. hex head bolts. Flat and lock washers were used throughout.

Ten-year zero maintenance was one of the design criteria.

2. Electrical

Typically, PV modules are rated under standard operating conditions (SOC). The following SOC is defined for the modules used in this system.

¹Array azimuth angle terminology used in PV engineering is also known as the wall angle in solar heating and cooling engineering. The angle will be referred to as the wall angle in this report and is simply the projection of the array normal to the horizontal plane. Angles east of south are positive, angles west of south are negative.

- (1) The module performance was determined when it was irradiated (illuminated) with 100 mW/cm² of an air mass 1.5 spectrum.²
- (2) The nominal operating cell temperature (NOCT) was defined to be 49°C (146°F) under no-load conditions when the air temperature was maintained at 20°C (68°F) with air motion of 1 m/s (2.2 mi/h).

Table 2 lists the performance of a sample module based on the above definition of standard operating conditions, and Figure 5 indicates the I-V characteristics.

As previously described, the modules were assembled as an array in an aluminum frame. Total module area is 3.7 m² (39.5 ft²). Within the array there is 2.37 m² (25.6 ft²) of active cell area. The ratio of module area to cell area is 0.65 for this array.

Figure 6 is an electrical schematic of the PV array. The last three digits of the serial numbers of each module are indicated and each module is numbered 1 through 22 in order to identify each protective diode in the diode box (described below). E-Z code tags are wrapped around each cable within the protective diode box. This identifies each module from the diode box and will allow quick module identification in the event of a module failure.

The protective diodes are silicon PN junction 1N4004 rectifiers. The purpose of these diodes is twofold. Figures 7(a) and 7(b) illustrate the use of

Table 2. Standard Operating Characteristics, PV System Module

POWER, MAXIMUM	10.1 WATTS
VOLTAGE AT MAXIMUM POWER	18.3 VOLTS
CURRENT AT MAXIMUM POWER	550 MILLIAMPS
VOLTAGE, OPEN CIRCUIT	22.5 VOLTS
CURRENT, SHORT CIRCUIT	620 MILLIAMPS
MODULE EFFICIENCY	6.1 %

²The sun's spectrum at the top of the atmosphere is defined as AM0. AM1 is the air mass penetrated by the sun's rays in the most direct optical path. Other air mass values indicate the ratio of the optical path length through the atmosphere to the path length through AM1 (Reference 2, Section 2.4). Therefore, different air mass ratios imply different shaped light spectra and therefore different module performance. The standard air mass 1.5 spectra is an analytically derived spectra (Reference 3) and represents the mean spectra of sunlight. For detailed information on the subject of performance reference conditions for PV array measurements, see Reference 4.

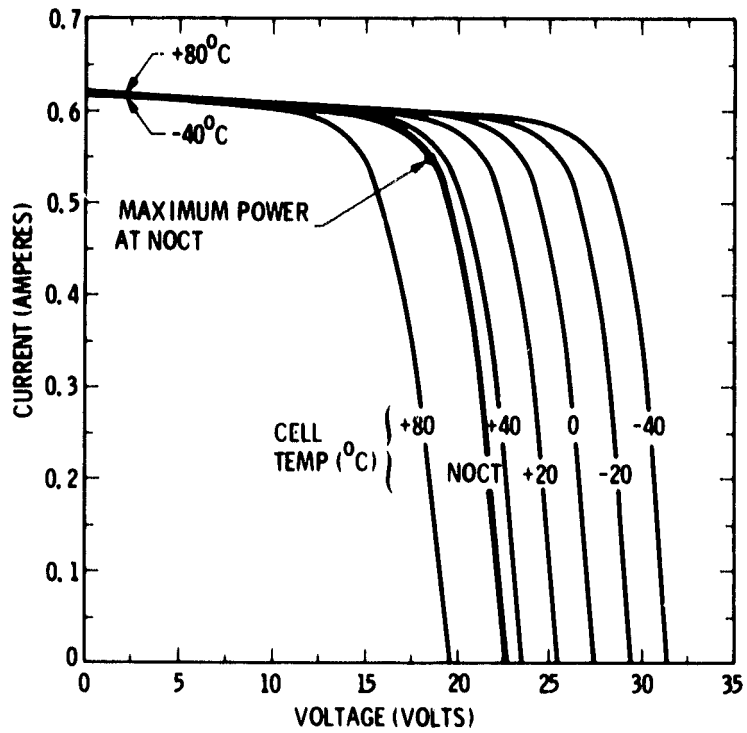


Figure 5. I-V Module Characteristics

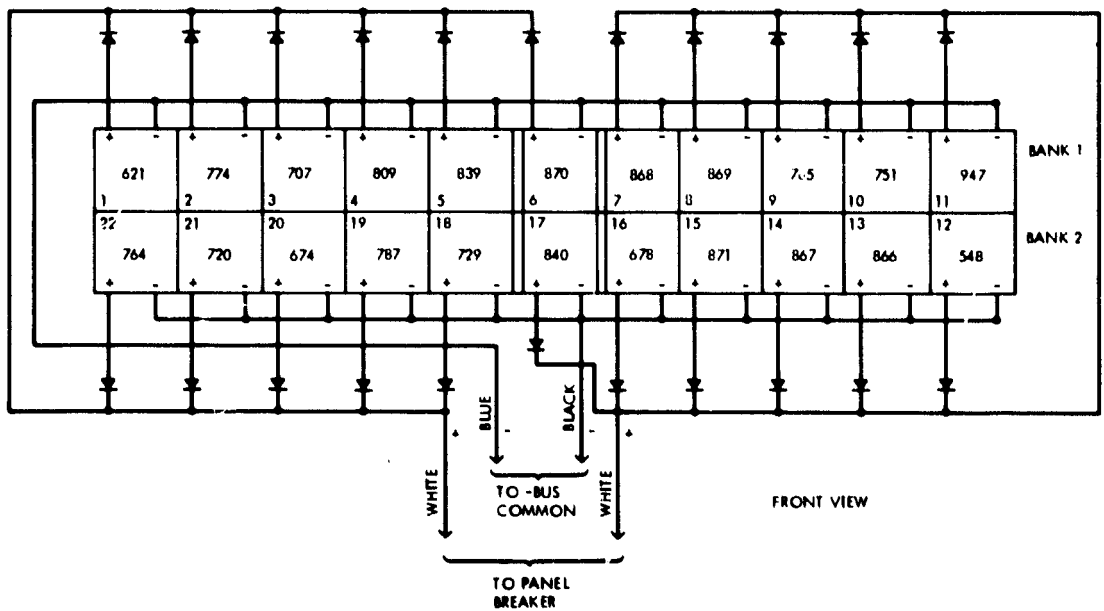
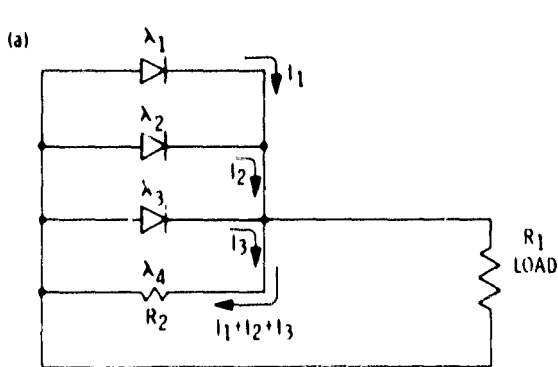
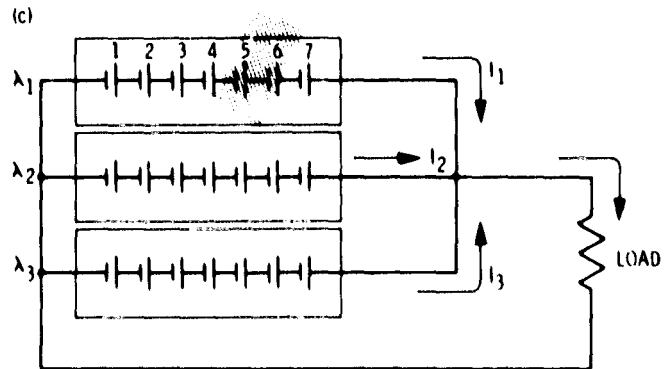


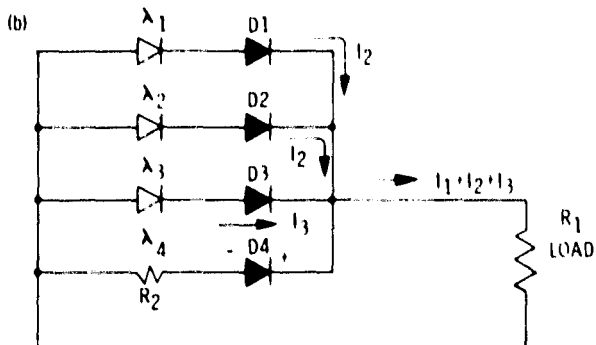
Figure 6. Schematic Diagram of a PV Array Configuration



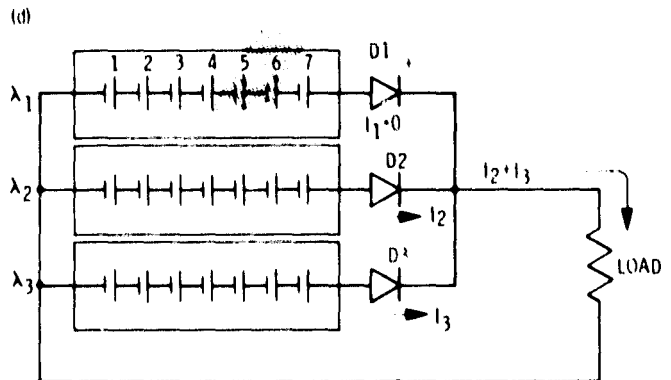
- IF $R_2 \ll R_1$, CURRENT FROM MODULES 1, 2, AND 3 WILL FLOW MOSTLY INTO SHORTED MODULE 4



- CELLS 5 AND 6 IN MODULE 1 ARE SHADOWED, RESULTING IN EXCESS HEATING FROM CURRENT PRODUCED IN CELLS 1, 2, 3, AND 4



- DIODE D4 IS BACK BIASED SINCE NO OR LITTLE VOLTAGE APPEARS AT SHORTED MODULE 4



- CELLS 5 AND 6 IN MODULE 1 ARE SHADOWED, WHICH PRODUCES A LOWER VOLTAGE THUS BACK BIASES DIODE D1 THEREFORE DIODE D1 CANNOT CONDUCT, PREVENTING CELLS 5 AND 6 FROM GETTING HOT

Figure 7. Protective Diode Applications: (a) Shorted Cells, No Protective Diodes; (b) Shorted Cells, Protective Cells; (c) Shadowed Cells, No Protective Diodes; (d) Shadowed Cells, Protective Diodes

these diodes in preventing good modules from being short circuited by a defective module. If resistance R_2 is much less than the load resistance R_1 , then current from modules 1, 2, and 3 will flow mostly into shorted module 4. Protective diodes (Figure 7b) will prevent this from happening. Figures 7(c) and 7(d) illustrate the same diodes being used to prevent potential problems from shadowing. Overheating can destroy cells or modules being shadowed or partially

shadowed. The unshadowed modules will effectively back bias the diode of the shadowed modules, thus preventing current flow and therefore preventing heat generation.

An alternative choice of diodes for these protective functions would have been Schottky-barrier type devices, which have a forward bias voltage drop less than that of a normal PN junction diode. Figure 8 illustrates the characteristics of the Schottky diode and Table 3 indicates the tradeoff and penalty for using both types of diodes for the system. The decision to use regular PN junction rectifier diodes rather than the more expensive Schottky diodes was based solely on cost for this system.

The diodes were mounted between solder terminals in a black painted metal box mounted underneath and always in the shadow of the array. To ensure that the diode matrix could dissipate about 8 W at high sun, holes were drilled in the top and bottom of the box to allow convection cooling. Water drip loops were formed

Table 3. PN Junction Versus Schottky Diode Trade-Off

DIODE TYPE	TYPICAL FORWARD VOLTAGE DROP	POWER LOSS AT 0.5 AMPS	TOTAL ARRAY POWER LOSS	UNIT COST (1981 DOLLARS)
P-N JUNCTION	0.70 VOLTS	0.35 WATTS	7.70 WATTS	\$0.44
SCHOTTKY	0.52 VOLTS	0.26 WATTS	5.72 WATTS	\$1.17

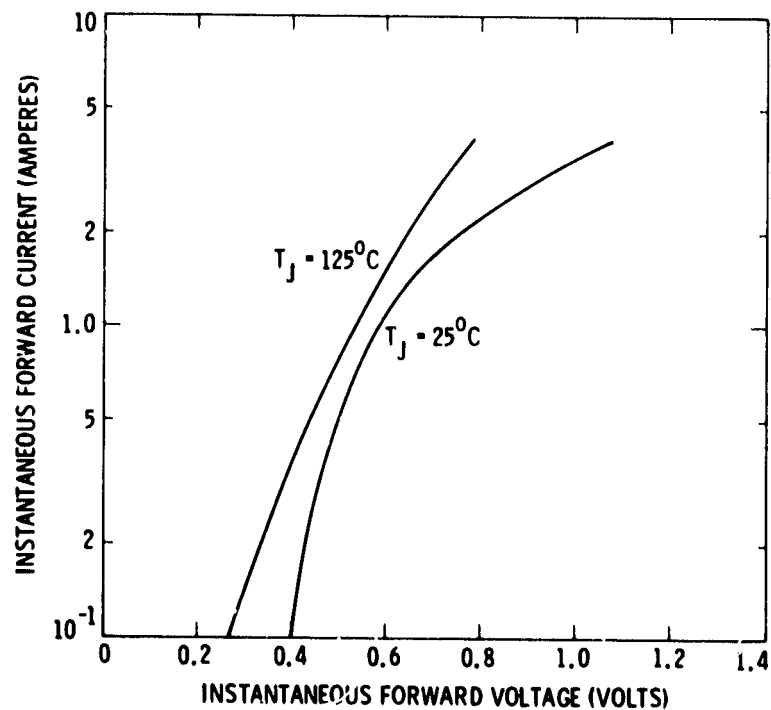


Figure 8. V-I Characteristics of Low-Current Schottky Diodes

on the input and output cables to keep rain water out of the box. The solder terminal strips were mounted on stand-off insulators and, if water should somehow get into the box, it will run out the bottom holes and won't get the diodes wet.

All the module "+" leads are connected to their diodes within the diode box and the cathodes of all diodes are connected together on a bus bar, thus effectively paralleling all "+" terminals of the modules. The modules' "-" leads are daisy chained together underneath the array, completing the parallel module configuration. Number 14 Teflon insulated wire was used throughout.

The PV array is physically divided into two banks of modules as seen in Figure 6. There are two reasons for this. First, the current path to and from the battery box (described later) could be divided into two loops, thus reducing the voltage drop in the cables and the associated energy loss. Second, comparison voltages and currents could be made at the battery box to determine the array performance. Differences will indicate a module performance problem. The two "+" leads are tied together at the PANEL circuit breaker in the breaker box, and the two "-" leads are tied together at an amp-meter current shunt where current comparisons between the two array banks can be made.

C ENERGY STORAGE AND REGULATION

1. Mechanical

An enclosure was constructed to house the batteries used for energy storage and the shunt regulator used for energy management. The enclosure is referred to as the battery box.

The battery box was constructed by pouring a concrete pad 145 by 43 cm (57 by 17 in.) and 20 cm (8 in.) deep just below ground level. 3/8 in.-16 by 6 in. bolts were inserted into the wet concrete so that 2- by 4-in. redwood studs could be anchored to the front and side perimeters of the pad to form a solid frame base.

Cedar grape stake was used to build a floorboard, allowing an air gap between the concrete surface and the top of the floorboard so that six 29-kg (65-lb) battery modules would be lifted up and off the concrete (see Figures 9 and 10). Any water entering the battery box will not collect around the base of the battery pack but will run out of the enclosure because of provisions made under the front side redwood base stud.

The front, sides, and roof of the box were constructed from 5/8-in. marine-grade plywood, which was waterproofed and painted before assembly. The front section measures 119 cm (47 in.) long and 50 cm (20 in.) high. A 3/4-in. dado was cut along the top edge so that the roof assembly would fit tightly over the front and sides. The sides were constructed in a similar manner and measure 74 cm (29 in.) long by 50 cm (20 in.) high. The roof measures 122 cm (48 in.) long and 86 cm (34 in.) wide and has a 13-cm (5-in.) overhang along the front to

ORIGINAL PAGE
BLACK AND WHITE PHOTOGRAPH

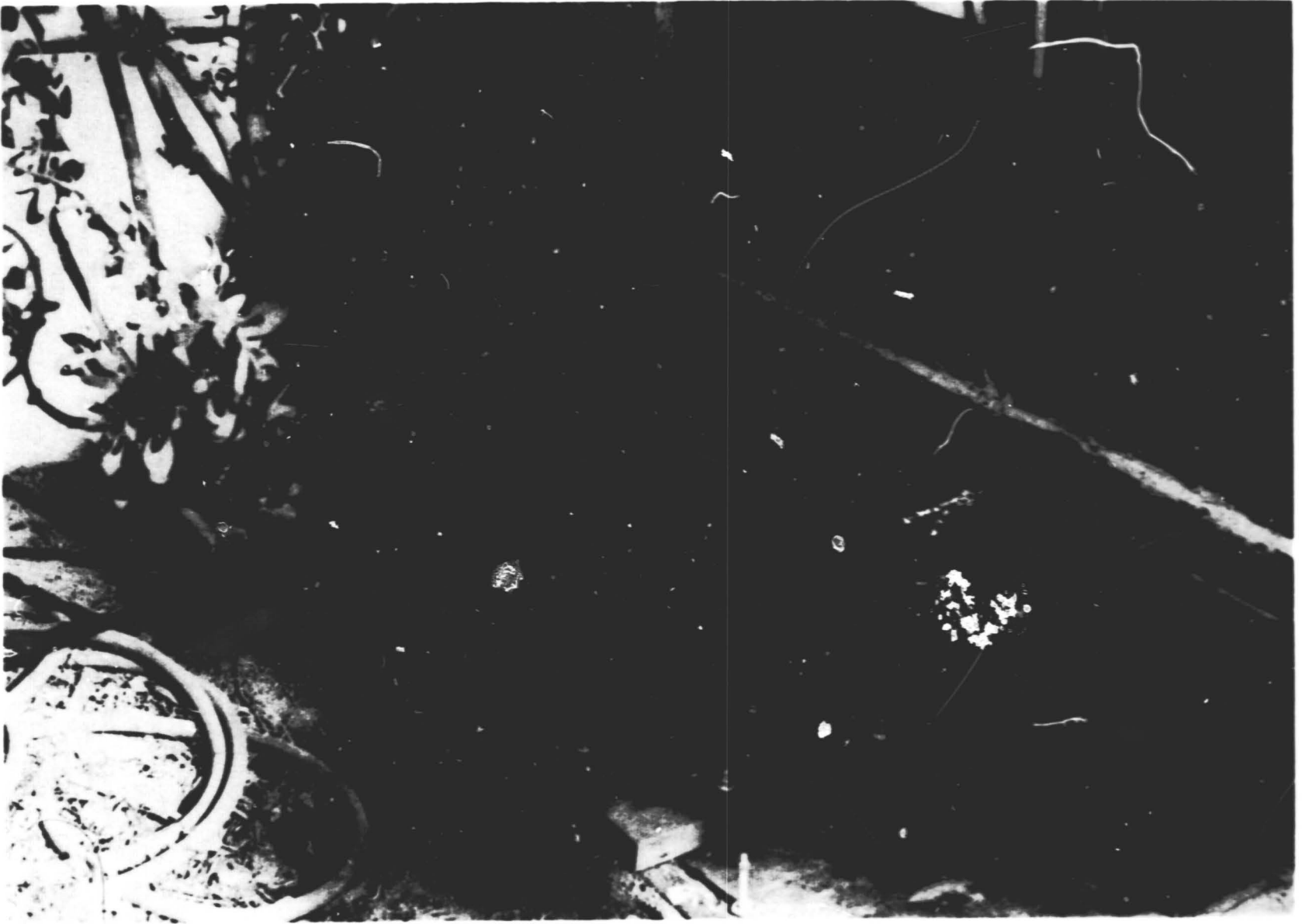


Figure 9. Battery Box Floorboard



Figure 10. Battery Modules on the Floorboard

prevent water from entering into ventilation areas. Dadoed front and side pieces were attached to the top of the roof to create a sloped roof and a tight seal around the edges of the roof interfaces.

Considerable design effort went into adequately ventilating the battery box. During battery charge, considerable hydrogen and oxygen can be produced and it is important to not allow an accumulation of these gases, particularly if electro-mechanical devices are used for inverter actuation and power distribution and management. Five large vents were placed in the front section of the box to provide 1045 cm² (162 in.²) of ventilation space, and two vents were placed on the one exposed side to provide another 290 cm² (45 in.²) of ventilation space. In the roof assembly, eighteen 2.5-cm (1-in.) holes were added around the front and sides to expel any gases that may collect against the inside top of the roof. Forty-four 0.64-cm (1/4-in.) holes were located in the back side in an area immediately above the heat sink area. Finally, all the rectangular vents were covered with aluminum vent mesh to prevent animals, including reptiles, from entering the box. Figure 11 shows the battery box enclosure.

All sections of the box were glued and screwed to provide maximum strength and rigidity and an expected zero maintenance (except perhaps for painting) 10-year lifetime. As a last measure, the roof was covered with a thin sheet of white fiberglass. During battery maintenance, the roof must be removed so it was desirable to keep it as light as possible.

2. Electrical--General

Access to the battery box is through holes in the back side panel. The four cables from the PV array enter the battery box and go to a breaker switchbox mounted on the outside front of the enclosures. The two positive leads are connected in parallel at the PANEL 15-A breaker. The output of this circuit breaker is connected to the +BUS IN bus bar inside the battery box. The negative leads from the PV array go into the battery box and are connected together at the AMP-HOUR METER SHUNT. A bus bar configuration is shown in Figure 12. There are three bus bars made of 3/16-in. copper bar stock, 5 cm (2 in.) wide. The bus bars are a convenient way of interfacing within the battery box. Also shown in Figure 12 are the forty-four 1/4-in. vent holes above the heat sink area (bottom), a Schottky isolation diode on a heat sink (upper left), and another Schottky isolation diode mounted on the +BUS OUT bus bar.

Figure 13 is a still more advanced conceptual diagram of this system. Extensive metering is indicated in this figure, along with circuit breakers and isolation diodes. The metering is used to obtain scientific and engineering data when the system is not being used for emergency drills and training. The first isolation diode after the array protective diodes is used to isolate the PV PANEL VOLTAGE meter from the rest of the system. This diode and the second isolation diode are Schottky devices whose forward voltage drops have been measured in the system at 0.35 V. Figure 14 indicates the V-I characteristics of these devices.

The metering is located on a specially designed silk screened panel that displays the conceptual system to the same extent as Figure 14.

ORIGINAL PAGE
BLACK AND WHITE PHOTOGRAPH

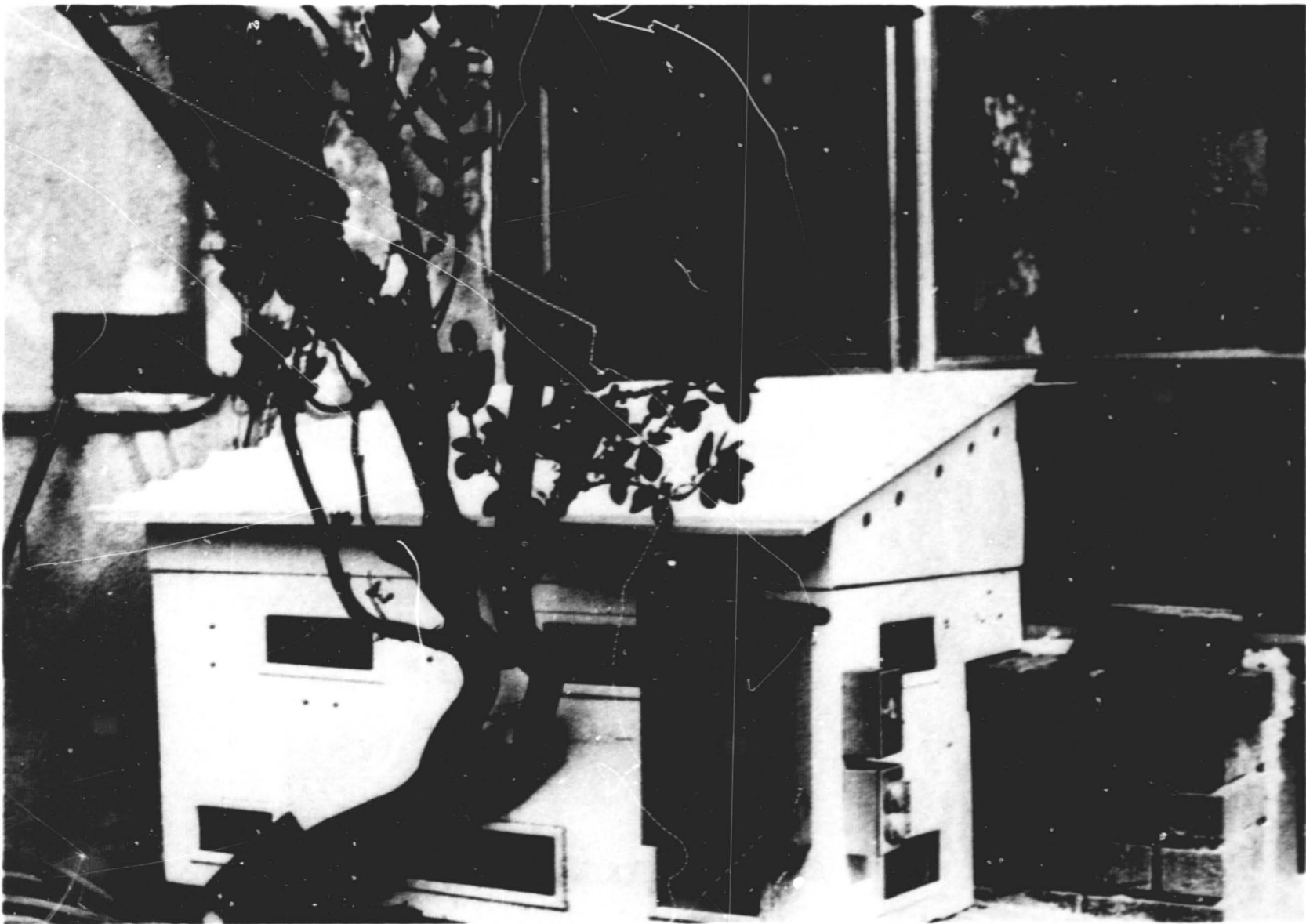


Figure 11. Battery Box

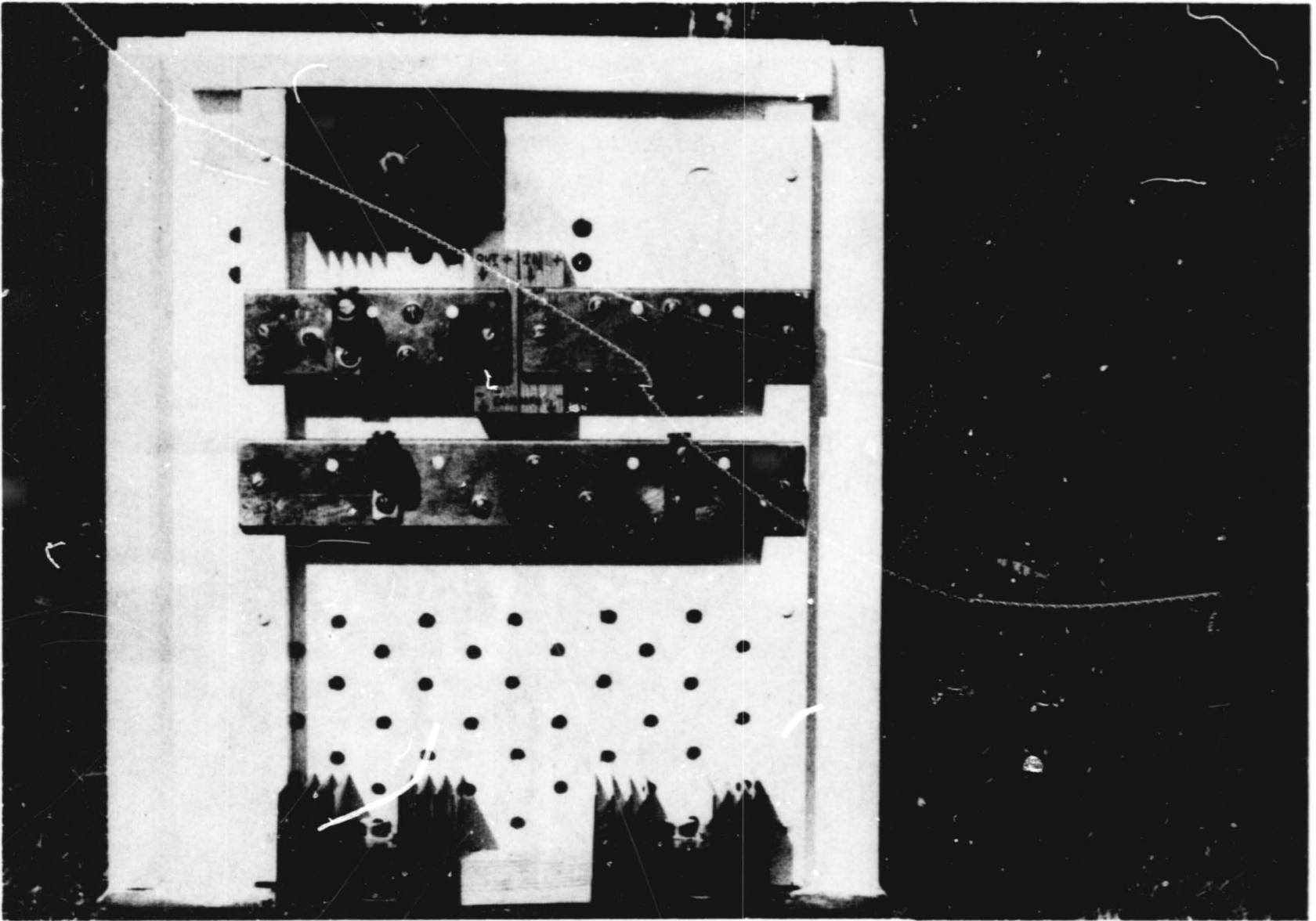


Figure 12. Battery Box Bus Bar Configuration

3. Shunt Regulator

Figure 15 is a detailed schematic of the system shunt regulator. A μA 723C integrated circuit regulator chip was used as the active device for the shunt regulator. The μA 723 is a monolithic voltage regulator constructed on a single silicon chip, using the Fairchild Planar epitaxial process. The device consists of a temperature-compensated reference amplifier, error amplifier, power series pass transistor, and current limit circuitry.

The 723 IC drives a pair of Darlington power transistors. These transistors are in series with the shunt resistors and regulate the current being shunted (diverted) away from the battery pack and load. These particular power Darlington transistors were selected because of their DC current gain versus collector current characteristics. Figure 16 illustrates these desirable characteristics (Reference 5). The current gain of these devices peak when the collector current is between 4 and 6 A. The DC current gain in this collector current range is about 175 at 25°C (77°F). The high gain (for a power transistor) is the result of the Darlington concept.

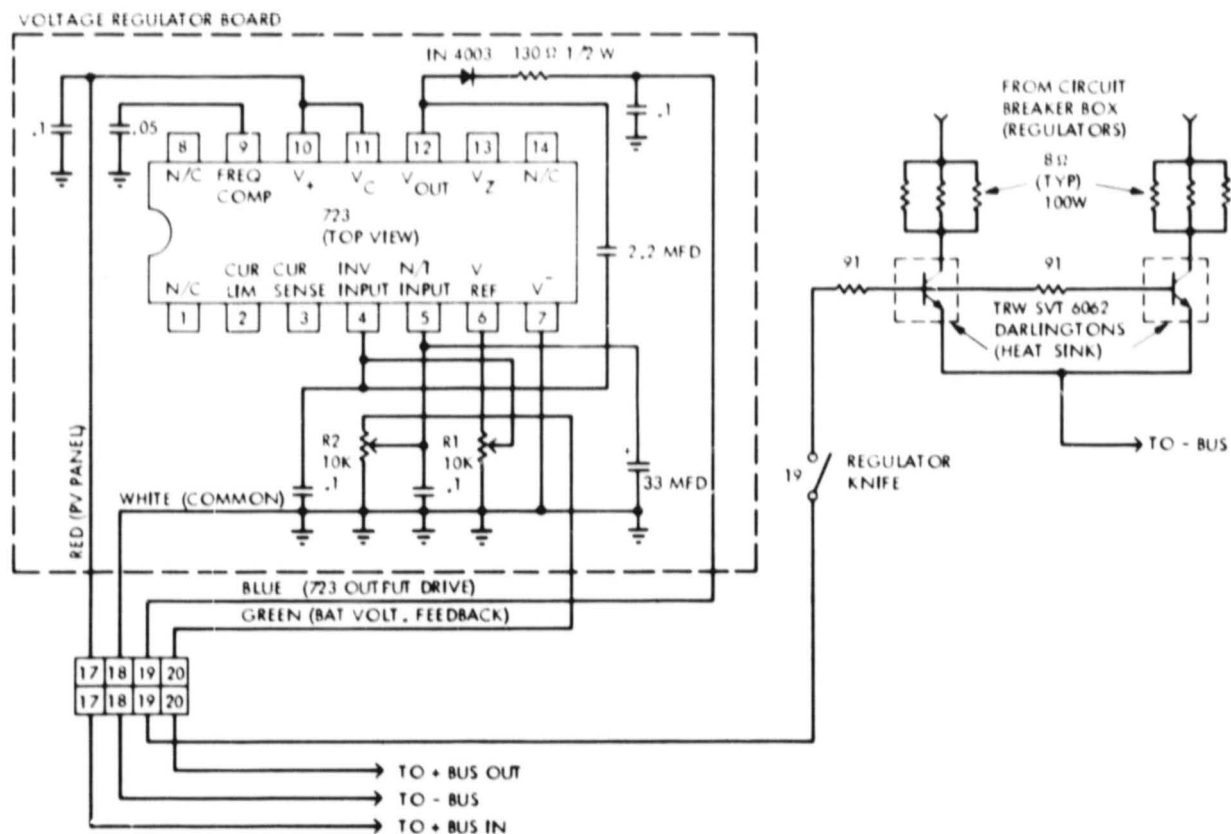


Figure 15. Schematic Diagram of a System Shunt Regulator

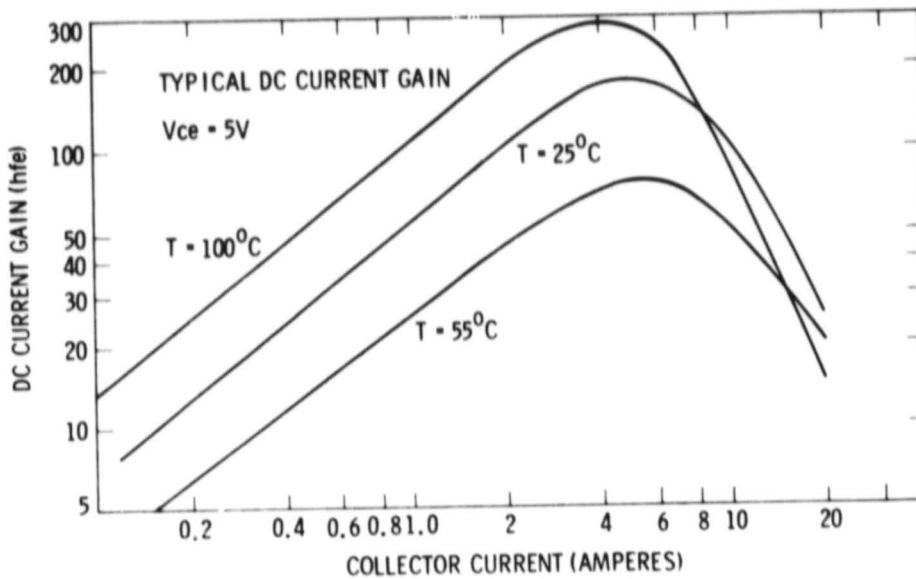


Figure 16. DC Gain Versus Collector Current, TRW SVT 6062 Darlington

Since the DC current gain is the collector current divided by the drive (base) current, it requires only about 23 mA of base current to conduct 4 A through each device. The 723 IC is capable of supplying at least 60 mA of drive current and is used to control two of these Darlington transistors, shunting at least 8 A of array current when the array current cannot be used in the system.

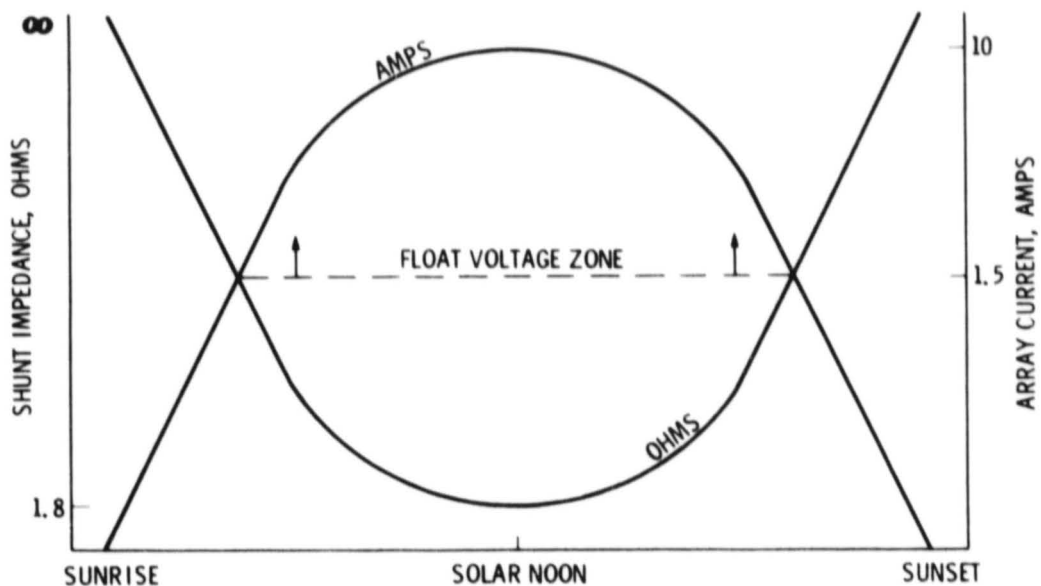
As less array current is needed to charge the battery pack and supply the load, more array current must be shunted in order to prevent overcharge of the battery pack and the resulting oxygen-hydrogen generation (electrolyte gassing or boiling). This means that the Darlington transistors must conduct harder, which implies that the regulator chip must supply more current to drive the transistors harder. At no time, however, are the transistors driven into saturation (full on), and the regulator chip drive current is limited by a 130-ohm resistor and also by a 91-ohm resistor in each base lead of the transistors.

As more array current is required to operate the equipment or maintain the battery voltage at float (that is, charge the battery pack), less current is needed from the system, and the transistors' drive currents are reduced accordingly, thus reducing their collector currents. If all or more than all of the array current is required by the load and battery pack, the shunt regulator turns off completely.

Control of the regulator is accomplished by a feedback loop that senses battery voltage. The regulator maintains the battery pack voltage and therefore the system voltage at the selected 14.1 float voltage during sun periods.

Severe instability problems were encountered until the bandwidth of the regulator loop was reduced to the point where the response time of the closed loop system was 1 or 2 seconds. This was accomplished by adding a 2.2 mfd capacitor (Figure 15) between the output and the inverting input of the 723 IC, and adding a 33 mfd capacitor from the noninverting input to ground. Commercially available regulator chips such as the 723 were designed for power supplies, not PV systems, and, in general, these devices are too sensitive for PV systems. Although not widely known, lead-acid batteries can respond at bandwidths up to 50 kHz to small current demands (Reference 6). The instability was caused by the high gain and wide bandwidth of the regulator chip and the wide response bandwidth of the battery system. The myth that the voltage cannot be changed instantaneously across a battery is not true if the changes are small in amplitude. The instability problem would not have been discovered if it had not been heard in the station communications receiver. An oscilloscope was then used to confirm the problem.

At sunup, the regulator is completely unloaded from the system and milliamps of current start flowing into the battery from the PV array. Refer to Figure 17. As the sun starts to cover more of the array, more current is produced and flows into the battery pack (under no-load conditions). The battery pack voltage starts to increase toward the float voltage level. As the array



NOTES:

1. CONCEPTUAL FUNCTIONS OF IMPEDANCE AND CURRENT
2. ASSUMES CLEAR DAY, NO SHADOWING, FULLY CHARGED BATTERY PACK

Figure 17. Shunt Impedance as a Function of Array Current and Float Voltage

puts out still more current and as the battery voltage gets closer to the float voltage, the shunt regulator impedance starts to decrease. There is a smooth, stable transition of current as the float voltage is achieved.

As the day approaches solar noon (Figure 17) more current is shunted through the regulator collector resistors and power transistors. Finally, as sunset approaches, the regulator impedance increases smoothly. Soon the array cannot produce enough current to maintain float voltage. At this point, all array current flows into the battery pack and none is shunted to ground.

The voltage regulator circuit board (Figure 15) is heavily bypassed with 0.1 mfd mylar capacitors to bleed off any rf which might ride into the regulator box through the cable harness.

The shunt resistors (collector resistors) consist of three 8-ohm, 100-W wire wound devices for each power transistor. The three resistors are connected in parallel (2.67 ohms) and, as previously indicated, function as the collector resistors for each power transistor.

The values of the collector resistors were selected to allow at least 4 A of collector current for each transistor. About two-thirds of the shunt power is dissipated in the resistors, allowing the power transistors to be operated in a rather conservative mode.

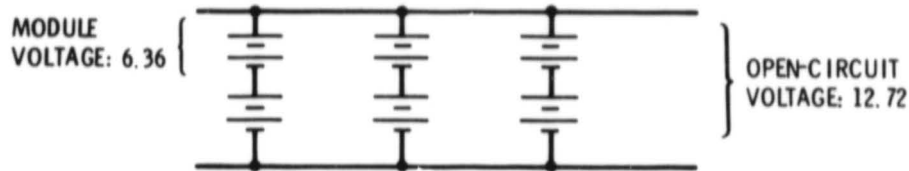
The physical location of the power transistors mounted on their heat sinks (Figure 12) is remote from their collector resistors. The resistors are mounted with stand-off brackets on the outside of the metal box containing the regulator circuit board. The transistors are on the opposite side of the battery box on heat sinks located at the bottom of the battery box where cool air next to the cement slab is available for convective cooling.

4. Battery Pack

The purpose of the shunt regulator is to prevent overcharging of the battery pack. The regulator guarantees a maximum system voltage. The 14.1 float voltage was selected for minimum positive grid battery corrosion (Reference 7) and thus for maximum battery pack life. As long as enough PV current is available, the shunt regulator will attempt to maintain 14.1 V across the battery pack.

The battery pack consists of six Exide EV IV nominal 6.36-V, lead-acid modules. These are identical electrically to the popular EV 106 golf cart battery. These modules are motive-type batteries in contrast to automotive lights, starter, and ignition-type batteries. The motive modules are designed for deep discharge-type service.

The battery modules are connected in a series parallel configuration to give a nominal 12.7-V, open-circuit terminal potential as indicated in Figure 18. Each module, by itself, is rated at 75 amperes discharge for 106 minutes, giving the entire pack a rating of about 400 amp-hours at a rate of 225 A.



TYPE: EXIDE IV (EV-106)
 LEAD-ACID (ANTIMONY)
 MODULE DIMENSIONS: 26.35 cm (10.375 in) L, 18.256 cm (7.188 in) W,
 28.813 cm (11.344 in) H

MODULE WEIGHT: 29.7 kg (65.5 lb)
 SPECIFIC GRAVITY RANGE-FULL CHARGE-22.2°C (72°F): 1.260 - 1.280

Figure 18. Battery Module Configuration

The actual amp-hour discharge capacity of these modules is a function of the rate of discharge and the electrolyte temperature and is given by the following model:

For $110 \geq I > 10$ amps

$$AH(I, ^\circ C) = kI^n [1 + 0.009 (^\circ C - 26.67)] \text{ amp-hours} \quad (1)$$

For $I \leq 10$ amps

$$AH(^\circ C) = 200 [1 + 0.009 (^\circ C - 26.67)] \text{ amp-hours} \quad (2)$$

where AH is the ampere-hour capacity available from the module as a function of discharge current I and initial electrolyte temperature (degrees Celsius).

The constants k and n are traditionally called the PEUKERT constants (Reference 8), but are nothing more than the curve fit coefficients to the power equation. At the temperature of 26.67°C and moderate currents between 10 and 110 A, the values of k and n are 438.63 and -0.2774 respectively (Reference 9). All of these constants have been determined for the type of module used in this system from actual laboratory tests. Equations (1) and (2) are battery constant current discharge models for the particular PV system batteries described. This model was used to help determine the number of parallel strings of modules required for this PV system.

Another laboratory-verified lead-acid battery model that was used to size the energy storage capability has been widely used in electric vehicle

simulation computer programs. First proposed by Brennard (Reference 10) and verified by Chapman (Reference 11), the equation is:

$$\ln P_D = A(\ln \tau)^2 + B(\ln \tau) + [C + \ln \{1 + 0.0063 (\text{°C} - 26.67)\}] \quad (3a)$$

where P_D is the constant specific power (density) discharge, in watts per kilogram of battery, and τ is the time to cut off, in hours, at constant specific power, P_D . The cutoff time is that time when the loaded battery voltage drops to the pre-agreed upon value that signifies "complete" discharge. At that point, the battery still has some capacity left, but it is that voltage point that was used to determine the constant power discharge coefficients in Eq. (3a).

The only solution (of τ) of interest from Eq. (3a) is:

$$\tau = \text{EXP} \frac{-B - \left[B^2 - 4A \left\{ C + \ln \frac{1 + 0.0063 (\text{°C} - 26.67)}{P_D} \right\} \right]}{2A} \text{ h} \quad (3b)$$

Again, °C is the initial electrolyte temperature and the A, B, and C coefficients are determined at 26.67°C . For the pack modules used in this system, the coefficients A, B, and C are -0.04113 , -0.69030 , and 3.08805 , respectively. These coefficients were determined from laboratory constant power discharge tests in contrast to the constant current discharge tests required to obtain Eq. (1).

The communications equipment and inverter appear neither as constant current nor constant power loads, but somewhere in between. Therefore, predictions from Eqs. (1), (2), and (3) represent probable bounds under which the batteries can be expected to perform.

Tables 4, 5, and 6 indicate the times to discharge expected of the battery pack based upon the type of duty cycles defined, the three strings of parallel

Table 4. Prediction of Battery Pack Performance: 50/50 Duty Cycle

	CONTINUOUS AVERAGE DISCHARGE REQUIREMENTS (EQUIPMENT)			TIME-TO-CUTOFF AT TEMPERATURE PREDICTIONS (h)			
	AMPS	SPECIFIC POWER watts/kg	AMP-HOURS PER 24 HOURS	CONSTANT CURRENT		CONSTANT POWER	
				4°C	27°C	4°C	27°C
LOW BAND	9.75	0.75	234	49	62	45	52
HIGH BAND	4.64	0.35	111	103	129	94	106
BOTH BANDS	14.39	1.1	345	33	42	31	36

Table 5. Prediction of Battery Pack Performance: 30/70 Duty Cycle

	CONTINUOUS AVERAGE DISCHARGE REQUIREMENTS (EQUIPMENT)			TIME-TO-CUTOFF AT TEMPERATURE PREDICTIONS (h)			
	AMPS	SPECIFIC POWER watts/kg	AMP-HOURS PER 24 HOURS	CONSTANT CURRENT		CONSTANT POWER	
				4 ⁰ C	27 ⁰ C	4 ⁰ C	27 ⁰ C
LOW BAND	7.65	0.59	184	62	78	57	66
HIGH BAND	2.86	0.22	69	167	210	145	168
BOTH BANDS	10.51	0.81	253	45	57	42	49

Table 6. Prediction of Battery Pack Performance: 10/90 Duty Cycle

	CONTINUOUS AVERAGE DISCHARGE REQUIREMENTS (EQUIPMENT)			TIME-TO-CUTOFF AT TEMPERATURE PREDICTIONS (h)			
	AMPS	SPECIFIC POWER watts/kg	AMP-HOURS PER 24 HOURS	CONSTANT CURRENT		CONSTANT POWER	
				4 ⁰ C	27 ⁰ C	4 ⁰ C	27 ⁰ C
LOW BAND	5.55	0.43	133	86	108	77	89
HIGH BAND	1.07	0.08	26	446	561	352	405
BOTH BANDS	6.62	0.51	159	72	91	66	76

modules, and two different electrolyte temperatures. For this design, the goal was to be able to operate for 72 hours in no-sun conditions assuming the 10/90 duty cycle. Equations (1), (2), and (3) were used to determine the number of parallel strings required using Table 1. The size of the PV array was based upon the battery complement.

Later, a structured methodology will be presented, using the equations just described to aid in specifying the battery pack amp-hour and energy capacity.

5. Battery Power Dissipation

The power dissipated in the battery pack is not the charge current times the float voltage. In fact, this calculation is not trivial except at the point where the battery pack is just fully charged.

The power dissipated in a lead-acid battery under charge conditions is:

$$q = (E_H - E_I) I \quad W \quad (4)$$

where

I is the charge current

E_I is the battery potential with I amps flowing

E_H is the thermal-neutral voltage

Consider Figure 19. The thermal-neutral voltage for any lead-acid battery is 2.07 V per cell when fully charged (Reference 12). Since 1.5 A is required to float the battery pack at 14.1 V when the pack is just fully charged, the power dissipated in the pack is (from Eq. 4) 2.52 W. Since the pack can only be charged until "full," the 2.52 W produces oxygen and hydrogen (known as gassing), which essentially causes the water to disappear from the electrolyte. The result of this is that water has to be periodically added to the pack. Continual charging beyond "full" (known as full overcharge) simply dissipates more power in the pack, and the additional energy from the array produces a pure electrolysis reaction, dissipating more power and producing more oxygen and hydrogen.

At night, with no current flowing into the pack, the pack voltage gradually drops. By sunrise, the pack is back to its open-circuit voltage, E_0 , assuming

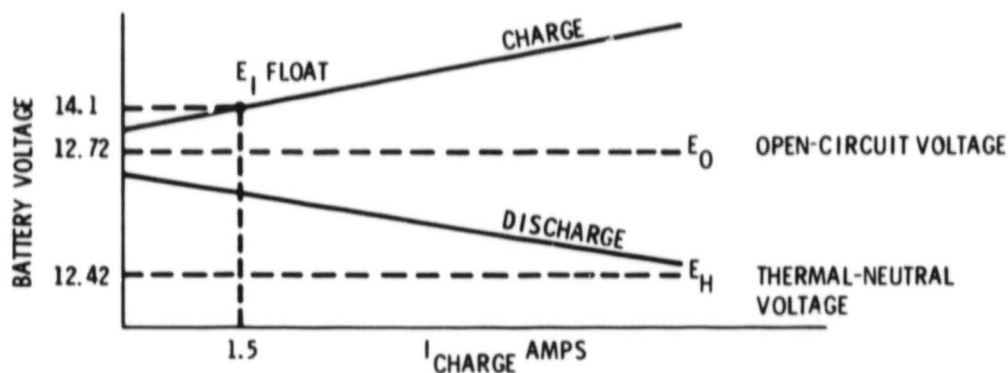


Figure 19. Relationships Among Float Voltage, Open-Circuit Voltage, and Thermal-Neutral Voltage

no energy was removed. It then requires more than 1.5 A initially to maintain the system voltage at float. In this system, it requires about 3 A for about one-half hour. Gradually, the current required to maintain the float voltage approaches 1.5 A, assuming no load.

The current required to maintain float voltage is electrolyte temperature dependent. The cooler the electrolyte, the less current required to maintain the float voltage. The exact relationships are unknown by these authors, but the temperature algorithms used in Eqs. (1), (2), and (3) do not apply. This temperature dependence suggests the fact that PV energy storage systems should be thermally managed (insulated) with provisions for gas management and automatic watering.

D. POWER CONVERSION

The system uses power conversion equipment to convert the nominal 12 V DC to 117 V AC, and 12 V DC to 700 V DC. The communications equipment will work on 117 V AC as well as on 12 V DC. The 117 V AC is required, however, to rotate the antenna arrays. In addition, the low-band equipment can run higher power output using 117 V AC rather than 12 and 700 V DC.

1. AC Inverter

A NOVA 5060-12 fixed frequency, sine wave, single phase inverter is used to produce 117 V AC from the system DC voltage. The inverter maximum continuous output rating is 500 VA. The device is voltage regulated to ± 1 percent for line or load and is frequency regulated to ± 0.15 percent for line or load. The manufacturer claims less than 5 percent maximum distortion. The efficiency of the inverter is about 60 percent.

The inverter can be actuated from the battery box or the radio room. It is actuated via a remote relay mounted in the battery box.

2. DC Converter

A DC-to-DC converter is used to supply high voltage to the final amplifier tubes in the low-band equipment if this equipment is used in the DC mode.

The DC-to-DC converter produces a chopped 100-Hz square wave, which is transformed to high voltage and then filtered. This converter will produce between 600 and 700 V and is not voltage regulated. Therefore, the input power to the low-band equipment is a function of the state of the battery pack. This converter is located in the radio room and is actuated by a switch on the low-band transceiver.

E. METERING

During the time that the station is not being used for training or drilling, engineering and scientific data are acquired for technical dissemination. This is accomplished by a complement of meters measuring various currents and voltages throughout the system.

Rather than limit the current and voltage monitoring to a few meters with a switching system for all necessary measurements, it was felt that simultaneous readings of various functions would be more desirable. Consequently, there are eight meters located on a meter panel displaying the system configuration (see Figure 20). Simpson Electric Company's 2½-in. Century Series meters were selected for most functions. Meter No. 1 (see Table 7) (0-25 V DC) continuously monitors the output of the PV panel, and Meter No. 2 (0-15 A DC) is in series with the PV panel output lead to continuously monitor current from the panel to the voltage regulator. Meter No. 3 (0-15 V DC) monitors the regulator output level, and Meter No. 4 (0-15 A DC) displays battery charge current. The battery pack voltage level is displayed on Meter No. 5 (0-15 V DC).

The three DC voltmeters incorporate Simpson's self-shielding annular, 1-mA movements which create 1000-ohm-per-volt sensitivity. This provides 24-hour-per-day monitoring with minimal power consumption from the meters themselves (3 mA maximum). The positive panel voltage circuit is fed through the system with diodes in series, where needed, to provide the necessary isolation to insure each meter's display is restricted to just its specified measurement task.

Meter No. 6 (0-30 A DC) is on the panel to display DC current being fed to the station operating room. Since an inverter is used to provide the needed 115-V AC power for the antenna rotator and other equipment, meters for monitoring its output are also provided. Meter No. 7 (0-5 A AC) monitors the current drawn from the inverter. Meter No. 8 (110-120 V AC true rms) was incorporated to monitor the inverter output voltage. The true rms sensing, along with the narrow voltage span of the meter, assures accurate measurements even if some sine wave distortion occurs.

Figure 21 indicates the wiring of these meters in the PV system. Each DC meter described above has an accuracy of 2 percent of full scale, and the AC meters are 3-percent devices. Table 7 lists the meter complement and manufacturers' identification information.

One more DC voltmeter is located at the station operating position where the operator can monitor the DC voltage level at the equipment location at all times and under varying loads. Its reading can be compared with the battery voltage level meter on the meter panel to determine exact losses (voltage drops) on the supply line to the station.

An amp-hour meter was built around the IMC Digital Ampere-Hour Integrator,³ Model 520, and this meter is used to measure amp-hours out of the PV array.

³International Microtronics Corporation
4016 East Tennessee Street
Tucson, Arizona 85714

Table 7. Meter Panel Complement

METER NUMBER	METER FUNCTION	MODEL	SIMPSON ELECTRIC	
			CATALOG NO.	RANGE
1	PV PANEL VOLTAGE	2122	17844	0-25 V DC
2	PV PANEL CURRENT	2122	17406	0-15 A DC
3	REGULATOR VOLTAGE	2122	17447	0-15 V DC
4	BATTERY CHARGE CURRENT	2122	17406	0-15 A DC
5	BATTERY PACK VOLTAGE	2122	17447	0-15 V DC
6	TOTAL LOAD CURRENT (DC)	2122	17408	0-30 A DC
7	INVERTER LOAD CURRENT	2152	17668	0-5 A AC
8	INVERTER OUTPUT VOLTAGE	3282	16295	110-120 V AC

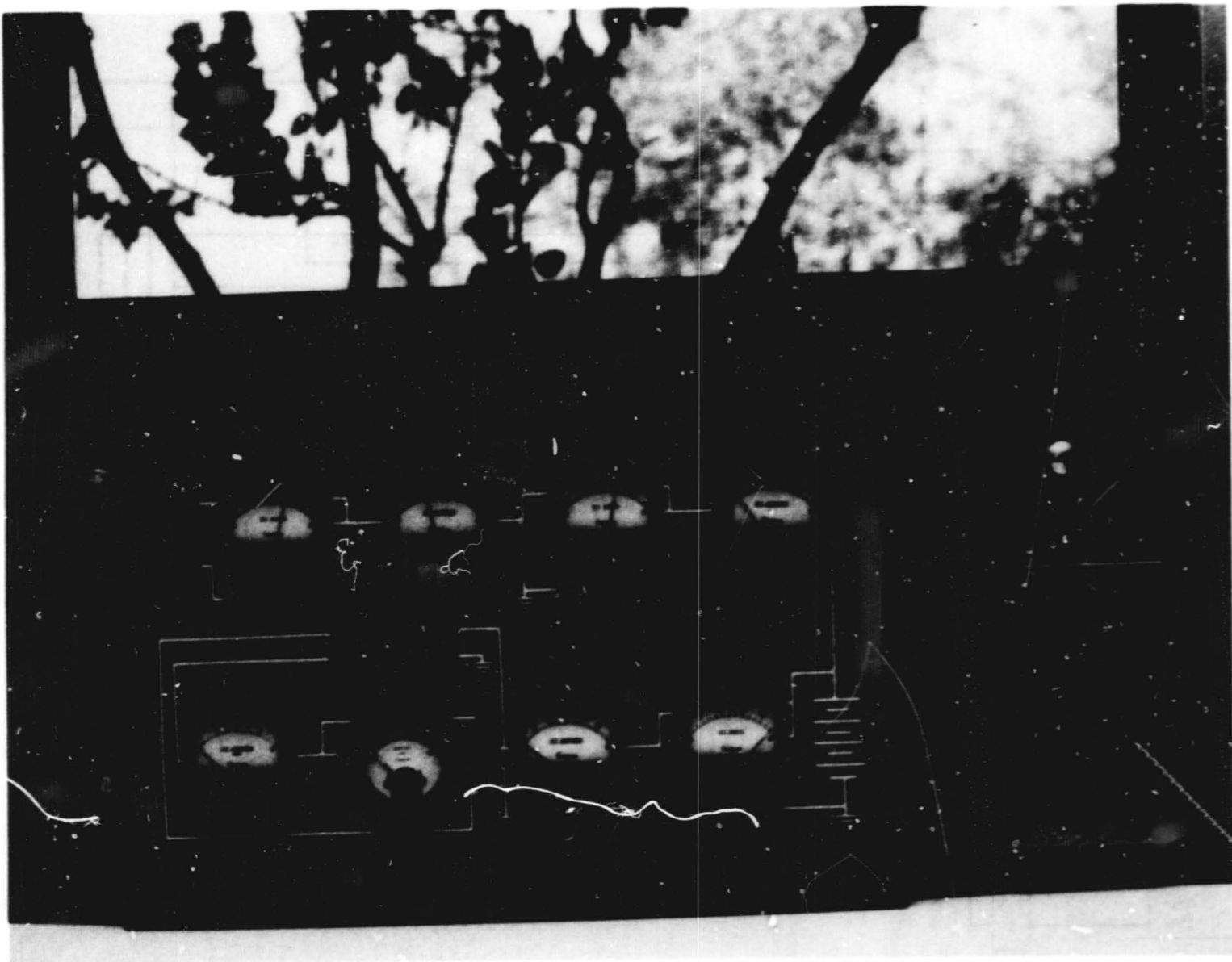
The IMC module consists of a voltage-to-frequency converter (VFC), a 4½-digit event counter, and a liquid crystal display (LCD). A highly stable operational amplifier amplifies the input signal and sends it to the VFC. The VFC output is a wave train of pulses whose frequency is proportional to the current. The input signal source is a 10-mV per amp, 1/4-percent precision current shunt located in the return lead to the PV array.

The array can produce over 10 A at high sun on a clear, cool day. Ten amps represents 100 mV across the current shunt resistor. If 10 A is maintained for exactly 1 hour, the amp-hour meter will read 100.0. When reading the meter, the observer must mentally move the display decimal point over one place to the left to convert the reading to amp-hours. This gives an accuracy to better than 0.1 amp-hour at any instant in time.

Since the pulse frequency from the VFC is proportional to array current at any instant in time, counting these pulses effectively integrates the PV current as a function of time.

The most significant digit of the 4½-digit display is either blank or a bar. Therefore, the maximum count is -999.9. The next increment of the counter will reset the device to 000.0. Thus, the device will measure 200 amp-hours before starting over. The device will hold the most recent count indefinitely under no-sun conditions.

Figure 22 is a schematic diagram of the amp-hour meter. The IMC module requires 9 V. A μ A 723C voltage regulator chip was used to regulate the battery pack voltage down to 9 V. The input to the voltage regulator can be any voltage greater than 11 V DC but less than 40 V. The meter requires less than 12 mA at 9 V.



ORIGINAL PAGE
BLACK AND WHITE PHOTOGRAPH

Figure 20. System Meter Panel

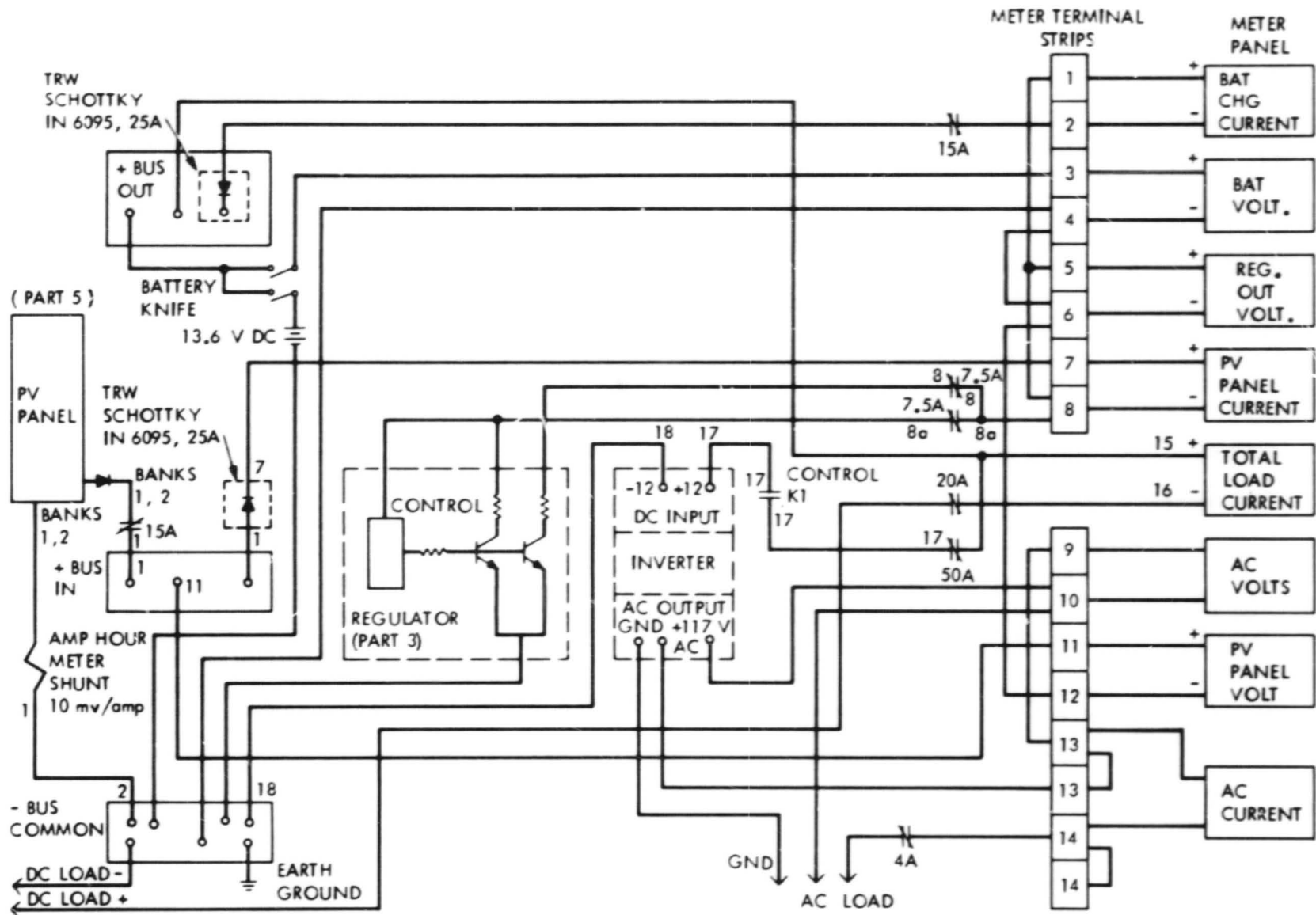


Figure 21. Meter Wiring Schematic Diagram

SECTION IV

ENERGY STORAGE SYSTEM DESIGN

A. STATION SYSTEM DESCRIPTION

The system elements of the station are shown in Figures 20 and 23 through 28. Figure 23 shows the radio room where the radio communications take place. Power distribution is controlled from here by sending electrical commands back to the battery box.

System interfacing occurs at the battery box. Energy is stored and allocated in the battery box. Figure 24 shows the bus bar interfacing. Energy storage and allocation is managed by the shunt regulator. Figure 25 shows the box containing the control electronics for the regulator and some of the shunt resistors used to dissipate excess energy when the energy cannot be utilized. The energy storage system and the device used to convert the DC power to AC power are shown in Figure 26. The breaker panel--an important safety feature even for low voltage systems--is seen in Figure 27.

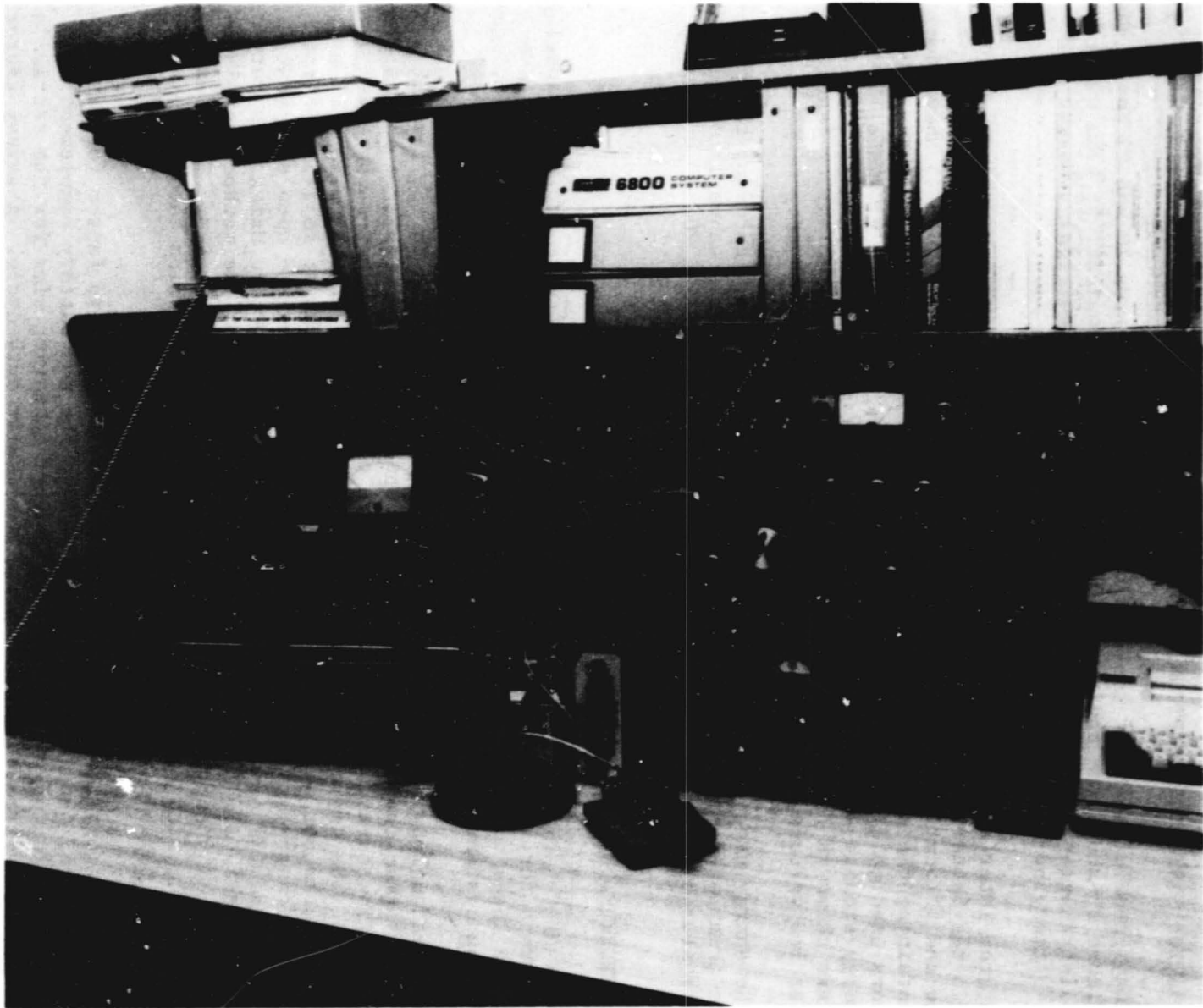
The energy used to operate the station equipment is collected by the photovoltaic array seen in Figure 28. And, finally, system performance is measured and indicated by the extensive metering system seen in Figure 20.

B. BATTERY STORAGE DESIGN METHODOLOGY

Some of the PV cell manufacturers have developed software tools for specifying PV arrays for systems requiring known or expected daily loads. Array systems whose loads are unknown and periodic are harder to specify. Emergency communications systems fall in this category.

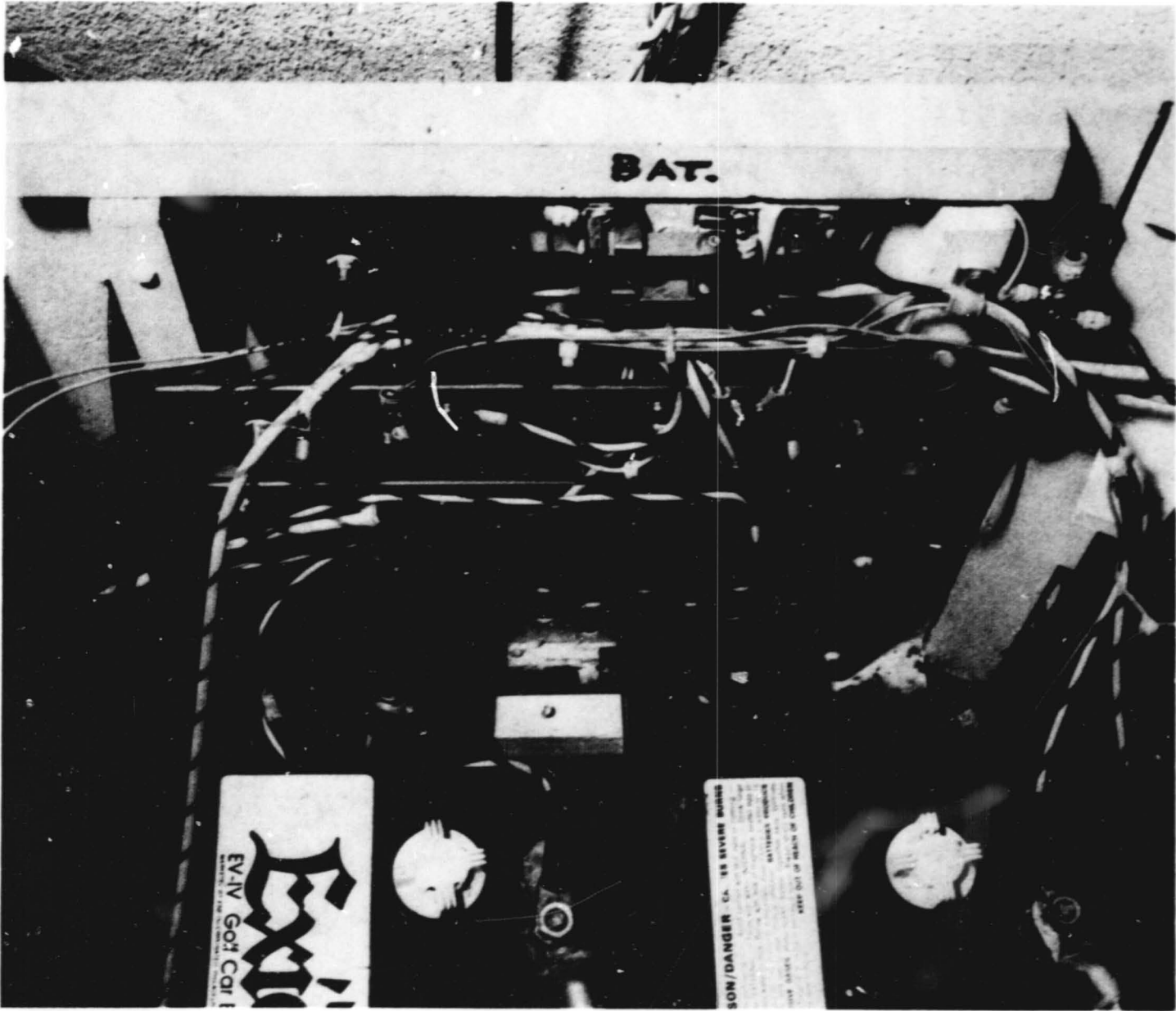
The methodology used to design this system is displayed in the form of a Nassi-Shneiderman chart in Figure 29 (Reference 13). These types of charts are similar to flowcharts but have the advantage of conveying precise concepts (structure). The key elements in designing an emergency communications PV system or any PV system not having a well-defined energy requirement is (1) to first determine the energy storage requirement based upon an agreed upon equipment duty cycle, and (2) to then determine a no-sun operating time using this duty cycle. Once these two critical decisions have been made, the methodology indicated in Figure 29 can be used to size the energy storage system. The PV array can then be specified by selecting a period of time over which the energy storage system must be capable of being recharged.

The methodology indicated in Figure 29 has no built-in factor for battery aging. Therefore, this methodology will yield the new battery complement to achieve a specified no-sun minimum temperature operating time for the station's average power requirements based upon a particular duty cycle. A safety factor and aging factor should be considered, which will result in at least one additional parallel battery string.



ORIGINAL PAGE
BLACK AND WHITE PHOTOGRAPH

Figure 23. Station Communication Equipment



ORIGINAL PAGE
BLACK AND WHITE PHOTOGRAPH

Figure 24. Bus Bars and Regulator Heat Sinks

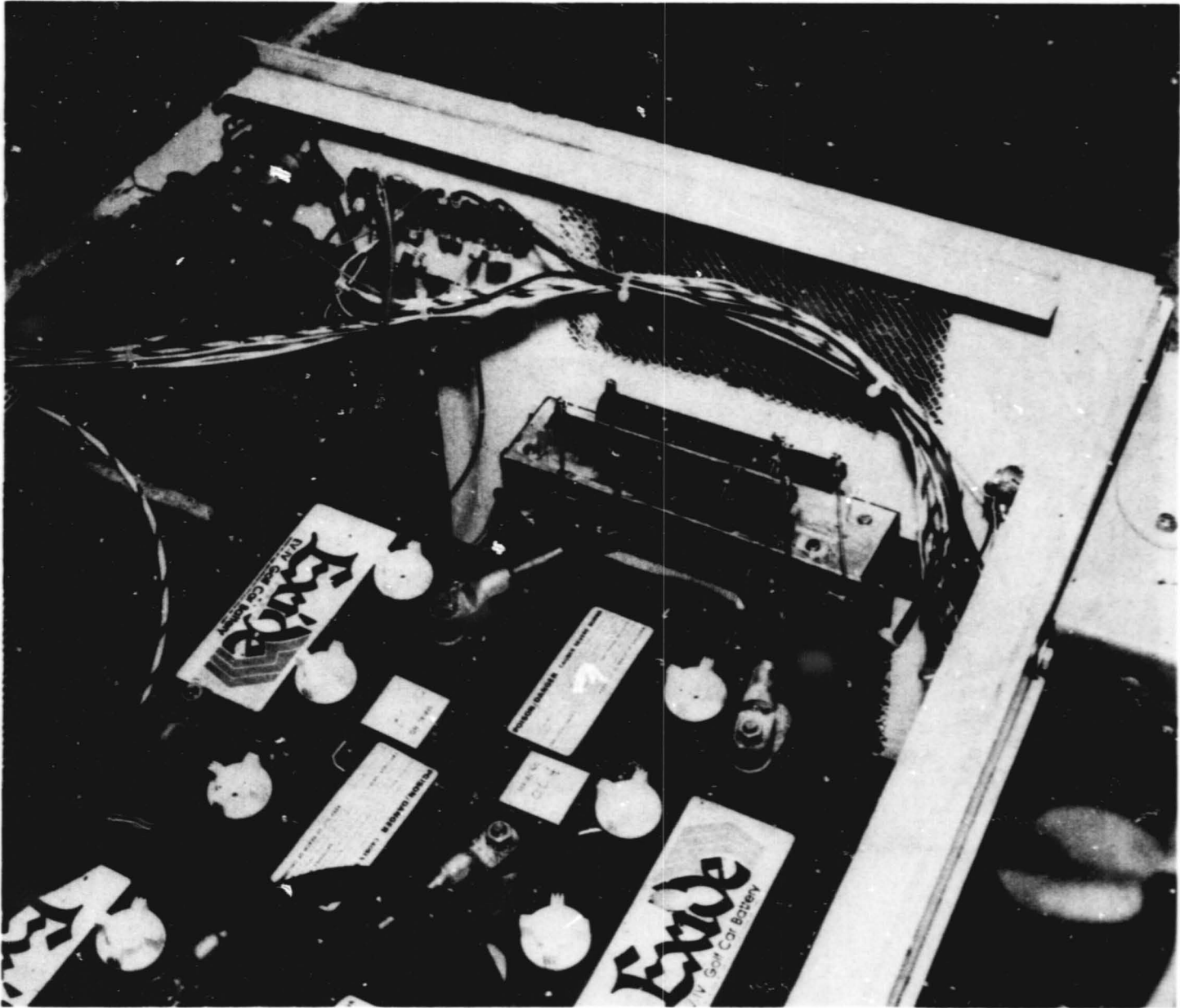


Figure 25. Batteries, Regulator Box, and Inverter Relay

ORIGINAL PAGE
BLACK AND WHITE PHOTOGRAPH

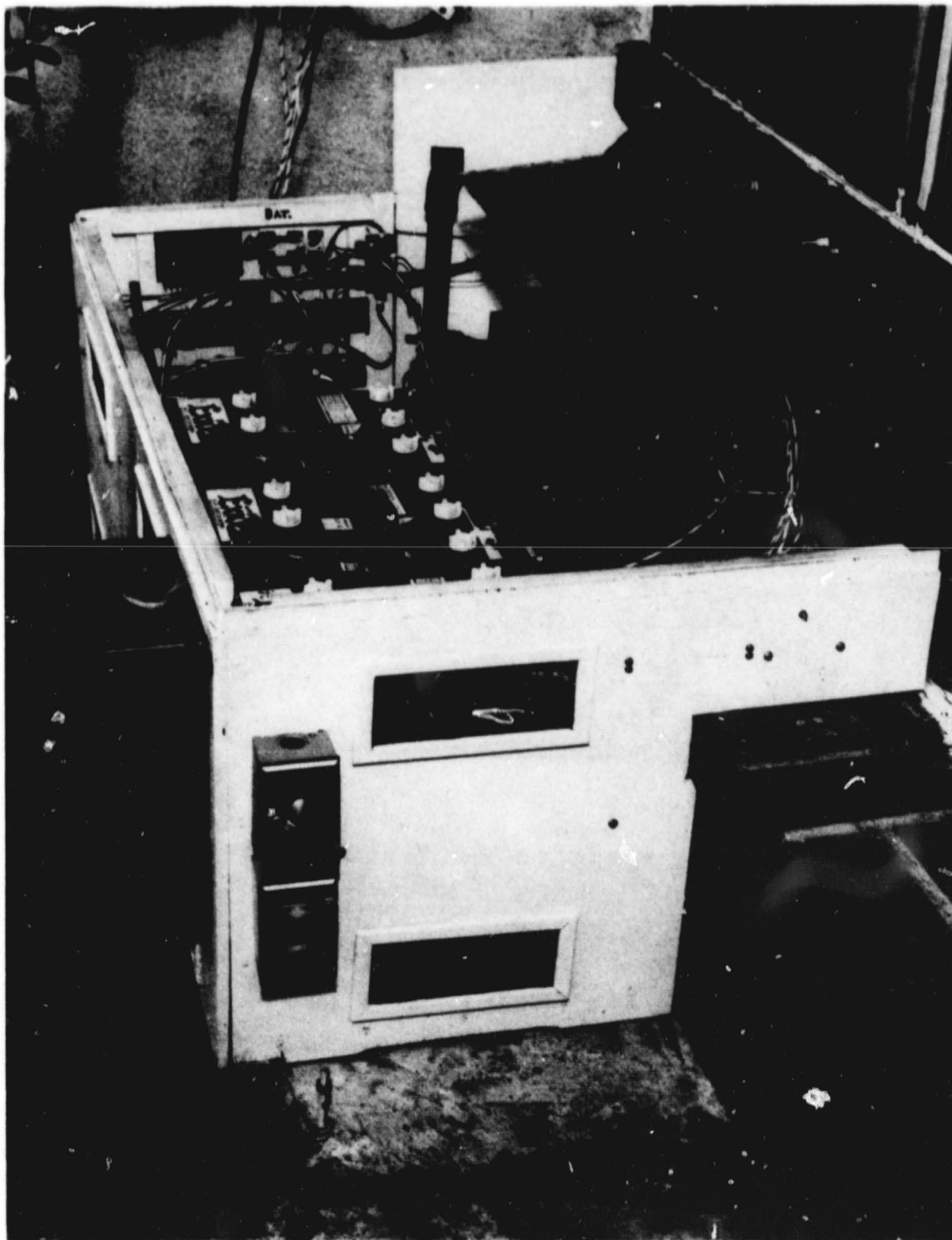


Figure 26. Batteries, Inverter, and Breaker Switch Box

ORIGINAL PAGE
BLACK AND WHITE PHOTOGRAPH

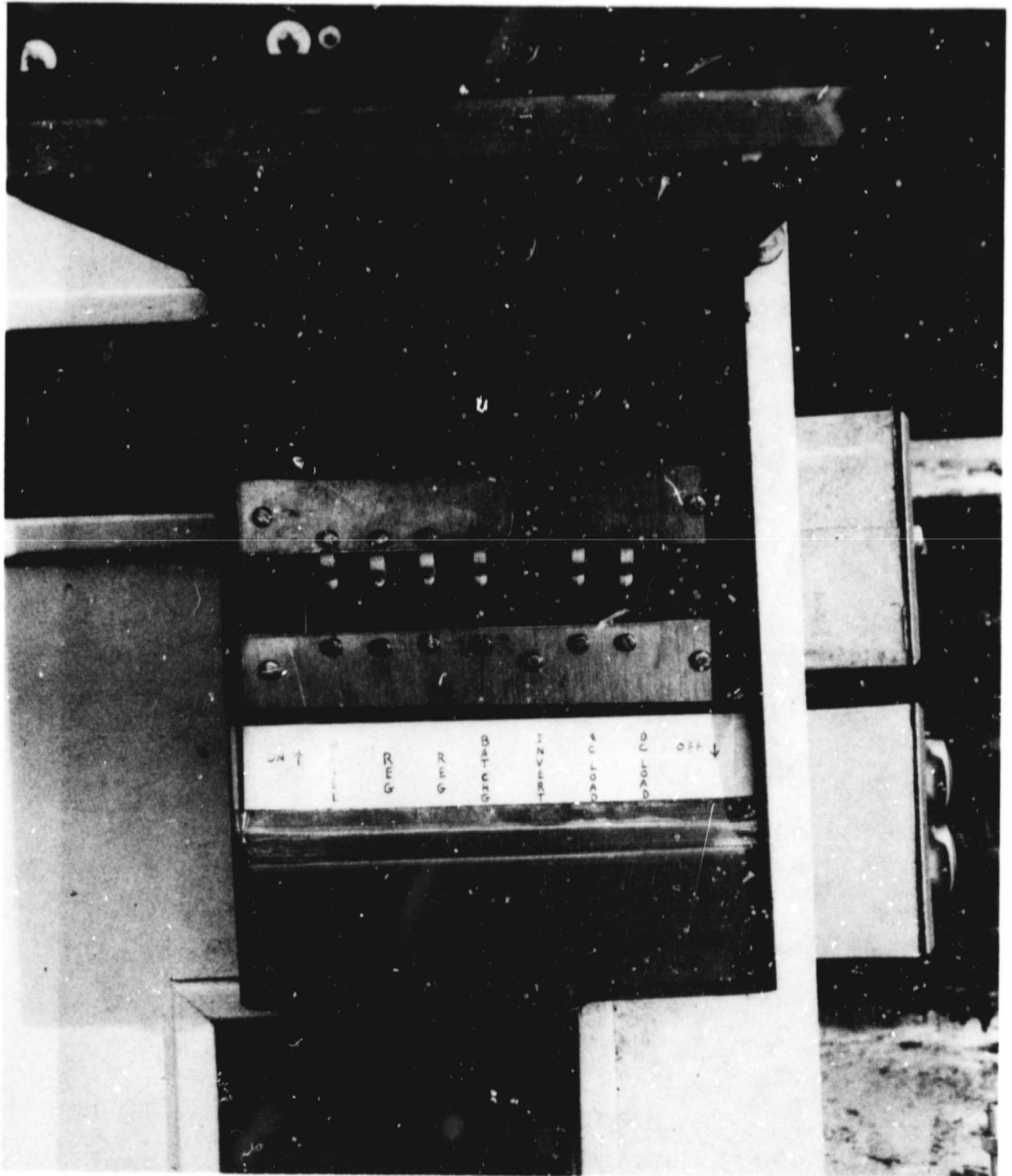
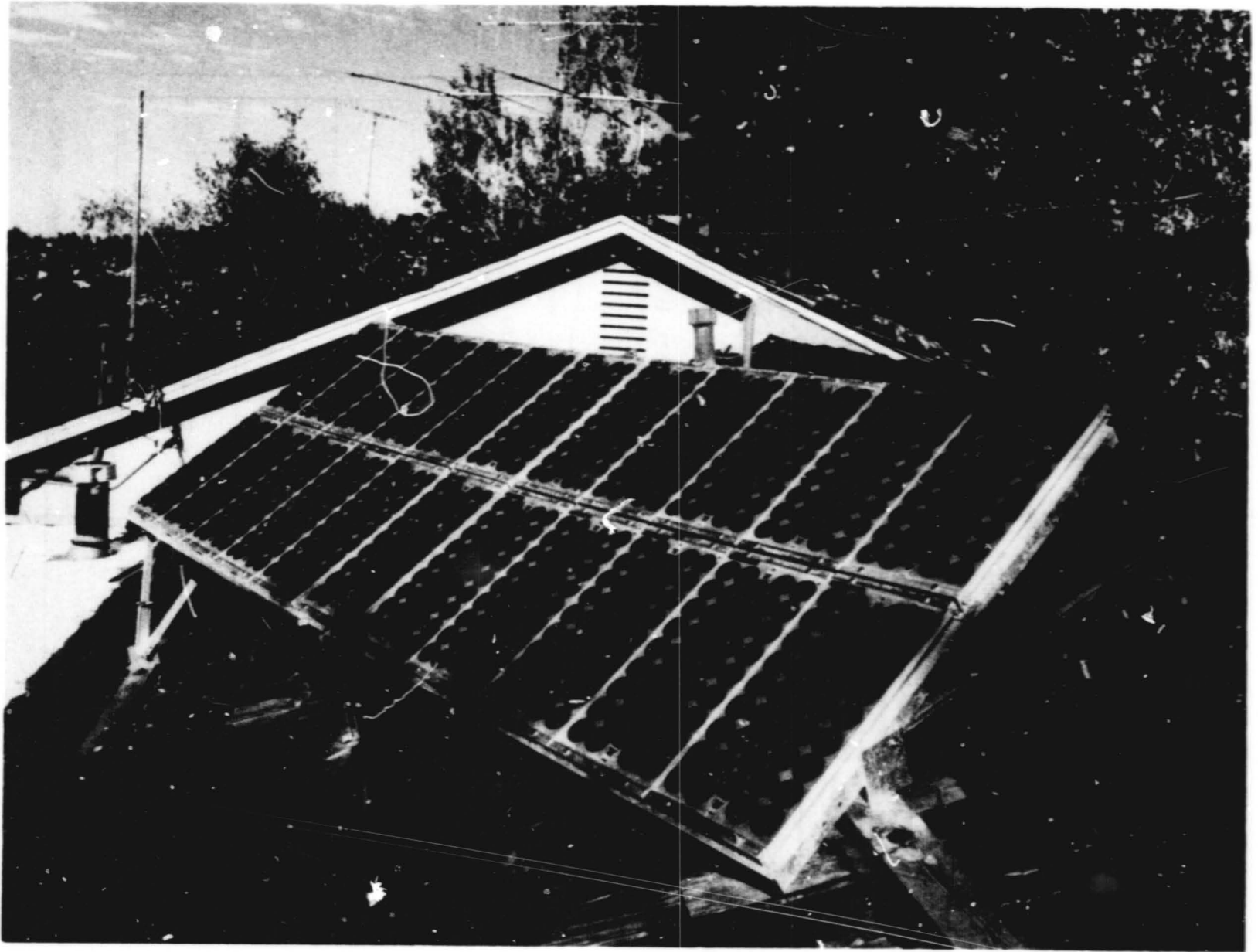


Figure 27. Breaker Panel



ORIGINAL PAGE
BLACK AND WHITE PHOTOGRAPH

Figure 28. PV Array

START:	BATTERY SIZING																			
LIST:	EQUIPMENT CURRENT REQUIREMENTS, I_{EQUIP}																			
SPECIFY:	DUTY CYCLE, NOMINAL DC SYSTEM VOLTAGE RX RECEIVE } FRACTION TX TRANSMIT } VDC																			
CALCULATE:	MAXIMUM AVERAGE EQUIPMENT REQUIREMENTS $I_{AV} = I_{EQUIP} \times RX + I_{AV} \times TX$ (AMPS) $P_{AV} = I_{AV} \times VDC$ (WATTS)																			
INPUT:	PEUKERT CONSTANTS; K, N REFERENCE TEMPERATURE: T_{REF} ($^{\circ}C$) C/20 BATTERY MODULE RATE: $c/20$ (AMPS) MINIMUM OPERATING ELECTROLYTE TEMPERATURE: T_{MIN} ($^{\circ}C$) BATTERY MODULE SERIES STRING WEIGHT: WT (KG) MAXIMUM NO-SUN OPERATING TIME: T_{MAX} (HR) CONSTANT POWER DISCHARGE COEFFICIENTS: A, B, C (AT T_{REF})																			
INITIALIZE:	J=1 COUNTER FOR # OF PARALLEL BATTERY MODULE STRINGS WB = WT PACK WEIGHT (KG)																			
DO	<table border="1" style="width: 100%; border-collapse: collapse;"> <tr> <td style="text-align: center;">THEN</td> <td style="text-align: center;">IF $I_{AV} \leq c/20$</td> <td style="text-align: center;">ELSE</td> </tr> <tr> <td colspan="2">$T_D = \{c/20 [1 + 0.009(T_{MIN} - T_{REF})]\} / I_{AV}$ HR</td> <td>$T_D = K I_{AV}^{N-1} [1 + 0.009(T_{MIN} - T_{REF})]$ HR</td> </tr> <tr> <td colspan="3">NOTE: T_D IS THE CONSTANT CURRENT DISCHARGE TIME, IN HOURS, AT CURRENT I_{AV} AND ELECTROLYTE TEMPERATURE T_{MIN}, $^{\circ}C$ USING J STRINGS OF PARALLEL BATTERY MODULES.</td> </tr> <tr> <td style="text-align: center;">THEN</td> <td style="text-align: center;">IF $T_D < T_{MAX}$</td> <td style="text-align: center;">ELSE</td> </tr> <tr> <td colspan="2"> $J = J + 1$ $I_{AV} = I_{AV} / J$ $WB = WT \times J$ </td> <td> $BAT_p = J$ NOTE: BAT_p IS THE NUMBER OF PARALLEL STRINGS OF BATTERY MODULES REQUIRED, OF TOTAL PACK WEIGHT WB KG AND I_{AV} AMPS FLOWING OUT OF EACH STRING. </td> </tr> <tr> <td colspan="3">UNTIL $T_D \geq T_{MAX}$</td> </tr> </table>		THEN	IF $I_{AV} \leq c/20$	ELSE	$T_D = \{c/20 [1 + 0.009(T_{MIN} - T_{REF})]\} / I_{AV}$ HR		$T_D = K I_{AV}^{N-1} [1 + 0.009(T_{MIN} - T_{REF})]$ HR	NOTE: T_D IS THE CONSTANT CURRENT DISCHARGE TIME, IN HOURS, AT CURRENT I_{AV} AND ELECTROLYTE TEMPERATURE T_{MIN} , $^{\circ}C$ USING J STRINGS OF PARALLEL BATTERY MODULES.			THEN	IF $T_D < T_{MAX}$	ELSE	$J = J + 1$ $I_{AV} = I_{AV} / J$ $WB = WT \times J$		$BAT_p = J$ NOTE: BAT_p IS THE NUMBER OF PARALLEL STRINGS OF BATTERY MODULES REQUIRED, OF TOTAL PACK WEIGHT WB KG AND I_{AV} AMPS FLOWING OUT OF EACH STRING.	UNTIL $T_D \geq T_{MAX}$		
THEN	IF $I_{AV} \leq c/20$	ELSE																		
$T_D = \{c/20 [1 + 0.009(T_{MIN} - T_{REF})]\} / I_{AV}$ HR		$T_D = K I_{AV}^{N-1} [1 + 0.009(T_{MIN} - T_{REF})]$ HR																		
NOTE: T_D IS THE CONSTANT CURRENT DISCHARGE TIME, IN HOURS, AT CURRENT I_{AV} AND ELECTROLYTE TEMPERATURE T_{MIN} , $^{\circ}C$ USING J STRINGS OF PARALLEL BATTERY MODULES.																				
THEN	IF $T_D < T_{MAX}$	ELSE																		
$J = J + 1$ $I_{AV} = I_{AV} / J$ $WB = WT \times J$		$BAT_p = J$ NOTE: BAT_p IS THE NUMBER OF PARALLEL STRINGS OF BATTERY MODULES REQUIRED, OF TOTAL PACK WEIGHT WB KG AND I_{AV} AMPS FLOWING OUT OF EACH STRING.																		
UNTIL $T_D \geq T_{MAX}$																				
CALCULATE SPECIFIC POWER:	$P_D = P_{AV} / WB$ (W/KG)																			
CALCULATE CONSTANT POWER DISCHARGE TIME:	$\tau = \text{EXP} \frac{-B - [B^2 - 4A \{c + IN \frac{[1 + 0.0063 (T_{MIN} - T_{REF})]}{P_D}\}]}{2A}$ HR																			
THEN	IF $\tau < T_{MAX}$	ELSE																		
$J = J + 1$ $I_{AV} = I_{AV} / J$ $WB = WT \times J$		END BATTERY SIZING																		

9/24/81

Figure 29. Battery Sizing Methodology

The aging factor for deep discharge lead-acid batteries is a function of the number of deep discharges experienced by the battery pack and the depth of these discharges and the operating electrolyte temperature environment. A discussion of expected battery life and aging is contained in Reference 14. In general, it is advisable to not allow the battery pack to drop below 50 percent of its full charge, if possible. This will extend the pack life by perhaps 40 percent in nominal temperature environments compared to discharges down to 80 percent of full charge.

Figure 29 indicates that the 20-hour current rating of the battery module must be known. This is designated as $C_{3/20}$ in the chart and is, in this case, referenced to the module 3-hour capacity which is designated as C_3 . For example, the 3-hour rate for the battery modules used in this system is about 50 A (i.e., $C_3 = 150$ amp-hours) so the $C_{3/20}$ rate is $50/20$ or 2.5 A. That is, the $C_{3/20}$ rate indicates that each series string of modules can produce 2.5 A of constant current for about 20 hours at the electrolyte temperature used to determine the 3-hour rate. Some battery manufacturers give a 20-hour rating for their batteries. Others give the time it takes to discharge the battery module at a constant current of 75 A. The C rating of a battery has units of amp-hours, and the C/20 or $C_{3/20}$ designation has units of current. The problem is knowing the time, in hours, that the module capacity has been specified. If the manufacturer indicates the 20-hour rate, then this current is used where indicated in the chart. If the time is not specified, an attempt should be made to determine the $C_{3/20}$ or C/20 rate. If the Exide IV or EV-106 batteries are selected as in this station design, then C between 150 and 200 amp-hours should be used. For very low currents (module currents less than 3.3 A), 200 amp-hours is probably more realistic in temperate zones.

The methodology of Figure 29 suggests knowing the constant power module discharge coefficients. These coefficients are time consuming to obtain, and only a few laboratories and manufacturers have the capability of obtaining this type of desirable information. This part of the methodology bounds the predicted discharge time of the battery pack. However, if the discharge coefficients are not known, then it will be necessary to neglect this part of the algorithm.

Following the steps in the chart will ultimately determine the number of parallel strings of batteries necessary to provide the required energy to operate the station for the specified number of no-sun hours with no safety margin or aging factor. At this point a decision must be made to determine how fast (in hours or days) the battery pack should be recharged after what is considered to be full depletion. Making this decision will yield the required array size in terms of required amp-hours.

For lead-acid batteries, amp-hours out of the battery is nearly equal to amp-hours in the battery. A conservative rule of thumb is:

$$AH_{\text{Charge}} = AH_{\text{Discharge}} \times 1.1 \quad (5)$$

For the station described in this report, a maximum of 10 full-sun days is required to fully charge the battery pack if the energy of the pack is

completely removed (80 percent depth of discharge) at the rate specified in Table 6. If this charge time were reduced in half, an array twice the size would be required.

C. CONSIDERATIONS FOR SPECIFYING RECHARGE TIME

The number of amp-hours per day of charge capacity available from an array on a cloudless day is a function of the:

- (1) In-system PV module current characteristics
- (2) Ambient temperature and atmospheric haze
- (3) Site elevation and latitude
- (4) Time of year (sun declination angle)
- (5) Array wall and tilt angles

The use of the PV module manufacturers' I-V characteristics may mislead the user. For example, on an average warm, mildly hazy 24°C (75°F) day at high sun, this system generates about 9.5 A with 22 modules in parallel which would indicate perhaps about 0.43 A per module. Allowing 2 V more above the float voltage of 14.1 V, the curves in Figure 5 indicate that the module current should be about 0.57 A, or 12.5 A total for 100 mW/cm² of sun radiation at the normal operating cell temperature. This may occur under special or ideal conditions, which is not most of the time. However, 80 percent of 12.5 A is 10.0 A, which implies that curves indicating 80 mW/cm² would probably be more realistic. In most instances where the SOC of the PV module is specified at 100 mW/cm² only, the actual performance will most likely be less than the I-V curves indicate with the modules in the system. In addition, the shunt regulator constrains the array voltage to 1 or 2 V above the float voltage, depending on the voltage drops (losses) between the array and the regulator. Therefore, the curves at 100 mW/cm² may not reflect the expectations of the actual system performance. However, an attempt has been made to correct this shortcoming (Reference 4).

Temperature and atmospheric haze affect the daily amp-hour totals, but not significantly over a several day period. Table 8 lists the amp-hours per day for this system for 20 consecutive days. Overcast or cloudy days swamp out the minor changes of temperature and haze as can be seen from Table 8. Neglecting days 12 and 18, the peak ambient temperature (high-to-low) changed by about 21 percent, but the array output only changed by slightly more than 6 percent (high-to-low). As the ambient temperature increases, so does the cell temperature. The short-circuit cell current increases less than 0.1 percent per degree Celsius with increasing cell temperature, but the open-circuit cell voltage decreases more significantly (2.2 to 2.3 mV per degree Celsius). The net result is a reduction in cell power between 0.3 and 0.5 percent per degree Celsius. The I-V curves translate up the current axis and shift to the left toward the current axis. The knee of the curve is purported to become more rounded (Reference 2, pp. 3.6-1-2). Assuming all the cell temperatures are the same in the array, the array temperature coefficients will have the same temperature

Table 8. Daily Array Output Versus Peak Ambient Air Temperature
(September 7-26, 1981, La Crescenta, California)

DAY	AMP-HOURS	TEMPERATURE		NOTES
1	57.62	32 ⁰ C	89 ⁰ F	
2	56.40	32	89	
3	56.89	31	88	
4	56.02	28	82	
5	56.45	29	84	
6	55.53	31	88	
7	55.55	29	84	
8	56.08	29	84	
9	56.74	31	87	
10	56.25	32	90	
11	55.23	33	92	
12	48.55	31	88	PART CLOUDY
13	56.12	32	89	
14	56.79	31	87	
15	57.24	29	84	
16	58.76	29	84	
17	57.75	28	83	
18	37.26	22	72	OVERCAST
19	55.12	23	73	HAZY
20	56.77	27	80	

relationships as the cells. Figure 30 indicates the temperature relationships at the cell level. In Figure 30, T is the cell temperature and T₀ is the cell reference (NOCT) temperature, in degrees Celsius. I_{sc} (T) and I_{sc} (T₀) are the short-circuit cell currents in amps at T and T₀, respectively, and V_{oc} (T) and V_{oc} (T₀) are the cell open-circuit voltages at T and T₀, respectively.

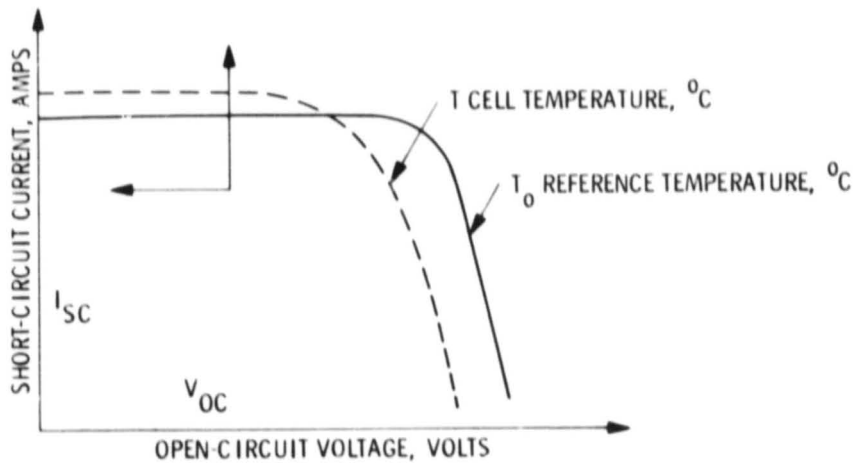
Haze affects the array output more than temperature (at least in temperate climates) as can be seen from comparing days 11 and 19 in Table 8. Table 9 compares an actual direct beam radiation measurement at the station site with three atmospheric haze models described in the Appendix. The radiation measured direct (beam) radiation of 82 mW/cm² where the haze model predictions varied between 65 and 96 mW/cm². This is indicative of the effects of haze versus array output.

The system described in this report has a fixed tilt angle of about 36 degrees and a wall angle close to zero degrees. The wall azimuth angle is the angle between true south and the array's surface normal as projected down to the horizontal plane. Wall angles east of south are positive, west of south negative. The tilt angle is positive for surfaces tilted generally upward and facing generally south. The tilt angle is zero for horizontal surfaces. Neither angle appears to be critical at nominal latitudes, particularly where a significant amount of the total irradiance falling on the array comes from reflections and diffuse reflections. If only direct beam radiation were available, the tilt

Table 9. Atmosphere Model Beam Radiation Prediction

MODEL HAZE	BEAM RADIATION, mW/cm^2		ERROR %
	PREDICTION	RADIOMETER	
23 km (14 mi)	91	} 82	11
5 km (3 mi)	65		-21
CLEAR	96		17

NOTES: JULY 16, 1981 DECL $21^{\circ}21'$ ELEVATION 0.38 mi ABOVE SEA LEVEL
 SOLAR NOON TILT 36° AMBIENT T 90°F
 LAT $34^{\circ}15'$ WALL 0° WEATHER HAZY



$$\beta_I = \frac{I_{SC}(T)}{I_{SC}(T_0) [T - T_0]} \times 100 \text{ SHORT-CIRCUIT CURRENT COEFFICIENT, } \%^{\circ}\text{C}$$

$$\beta_V = \frac{V_{OC}(T) - V_{OC}(T_0)}{T - T_0} \text{ OPEN-CIRCUIT VOLTAGE COEFFICIENT, VOLTS}^{\circ}\text{C}$$

*FROM (2), PP 3.6-1, -2

Figure 30. Temperature Effects on Cell Performance

angle would be more important. A tilt angle near the site latitude appears reasonable for fixed tilt angle installations such as this system.

The sun's declination angle or time of year is important to the extent of establishing the number of hours the sun is available to irradiate the array. This is implicit in what is called the solar hour angle, which is equal to 15 degrees times the number of hours from local solar noon. In the summer the array will produce more daily amp-hours simply because the days are longer, and, in the winter, fewer amp-hours. This must be considered in specifying the array to recharge the battery pack in a given number of hours or days.

Figures 31 and 32 indicate the array current performance over a single cloudless day. The data used to obtain these figures was taken on September 7, 1981 at the site. The peak ambient temperature reached 32°C (89°F). Some partial shadowing from a tree occurred in the late afternoon, which caused the rather steep slope between 8.5 and 9 hours from sunrise in Figure 32. The shape of these functions are characteristic of fixed wall and tilt angle PV systems. The functions can be described mathematically, which is one method of characterizing and comparing PV systems as a function of time-of-year and hours from sunrise. For example, this system can be described on a daily basis during at least a 30-day period between August 15 and September 15 (assuming clear skies) by:

$$AH = 1.90 - 4.65 t + 2.59 t^2 - 0.156 t^3 \text{ amp-hours} \quad (6)$$

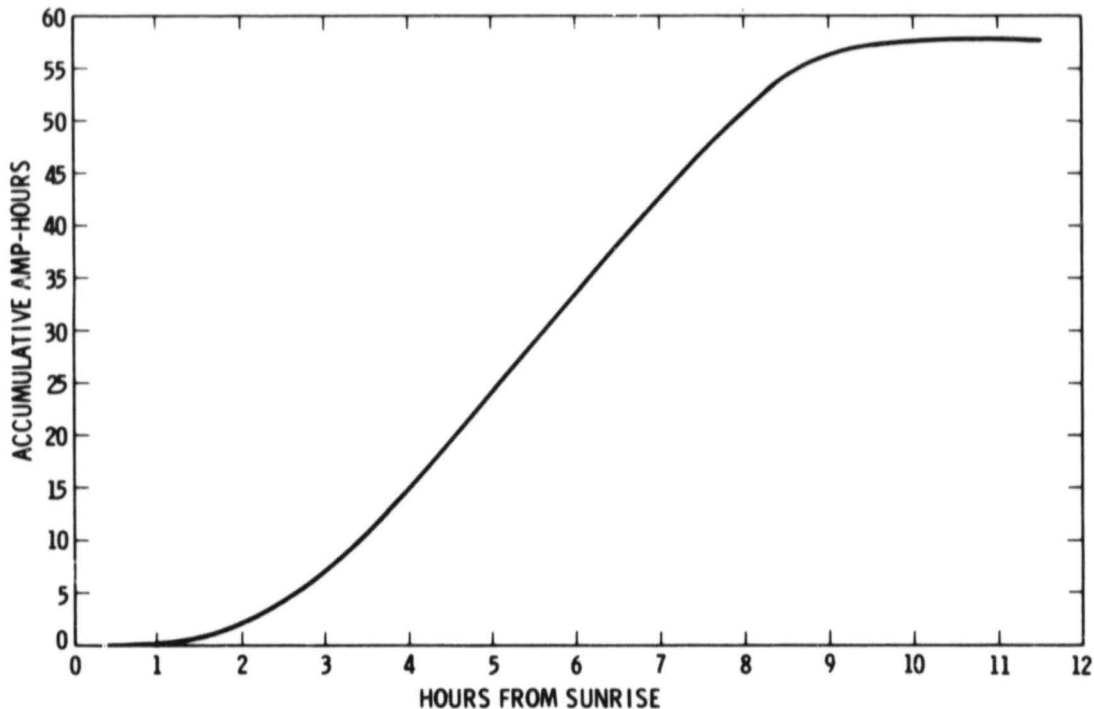


Figure 31. PV System Accumulative Amp-Hours Function

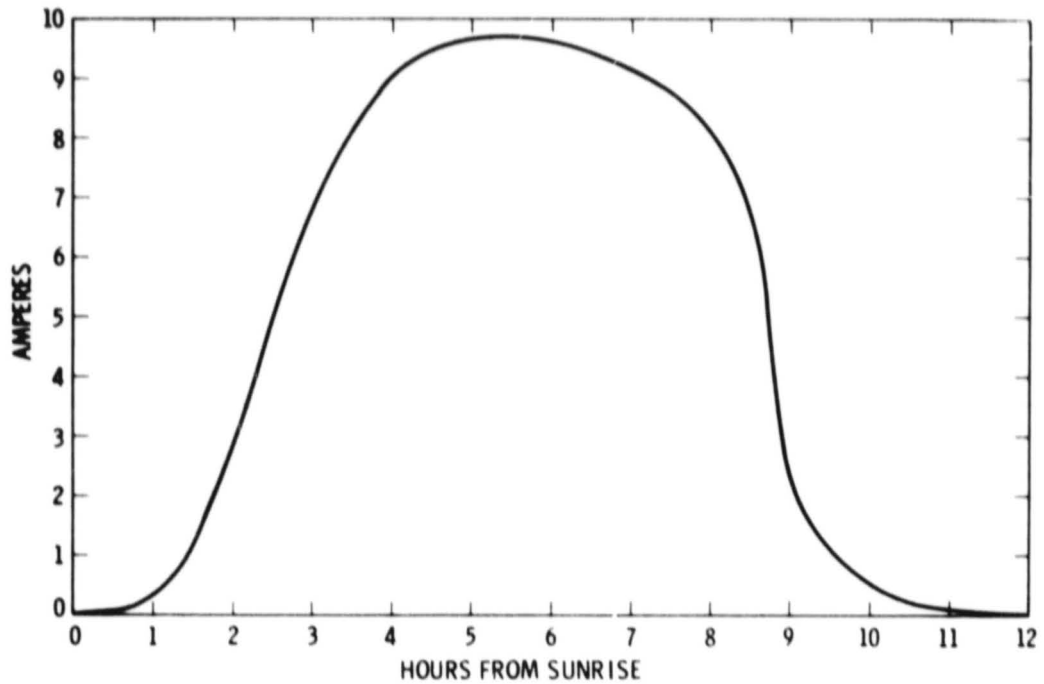


Figure 32. PV System Array Current Function

where

t = time, in hours, from sunrise

AH = the daily accumulative amp-hour capacity available from the array for operating equipment or storage, or both.

Restricting t between 2 and 11 hours after sunrise will give array description accuracies better than 3 percent over most of each clear day during at least the 30-day period.

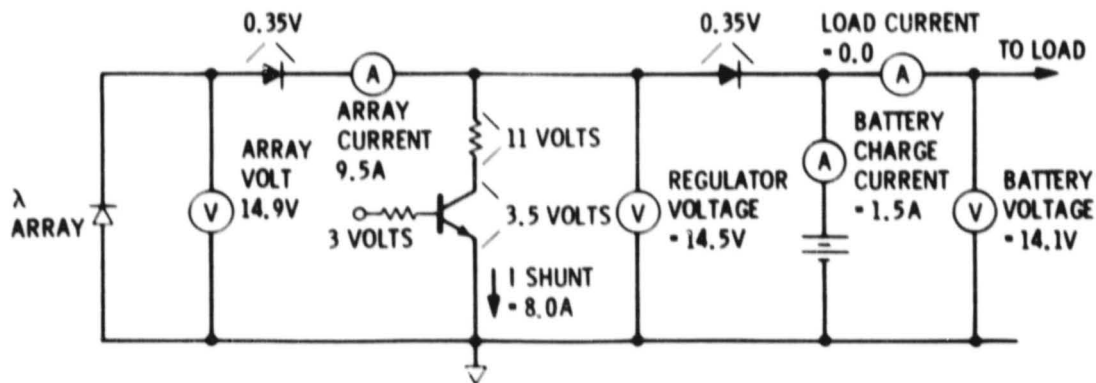
SECTION V

ENERGY DISTRIBUTION SYSTEM

Figure 33 indicates the nominal voltages and currents from the PV array and within the battery box at high sun. The battery pack is assumed to be fully charged with no current being drawn from the radio equipment. The radio room is electrically connected to the system illustrated in Figure 33 by two copper stranded #4 weld cables for the DC loads, two copper stranded #12 cables for the AC loads, and one #14 wire for inverter control.

A. GROUNDING SYSTEM

The system ground is established at the battery box where the negative side of the battery pack (the bus bar) is connected directly to the utility company ground. However, this is not a single point ground since the radio tower and yagi antenna systems are grounded via the tower base, which itself is 5 ft in the ground. The outer shields on the coax cables connecting the radios to the antennas are at ground potential because of a radio room ground system used when operating the equipment from utility company power. This ground is the same ground at the battery box but not the same point ground. Therefore, this system has a known 3-point ground configuration which was initially of some concern. However, although less than desirable practice, no problems exist and, with all the equipment operating in the solar power mode, less than 2 mA of ground loop current has been measured. It is important, however, to keep the DC current meters in the current source side of the equipment, rather than what is believed to be the current return (low) side when single point grounding cannot be used. Otherwise, the meters may not read correctly. In short, single point grounding is not necessary. The station has been operated partially on utility power, some



NOTES:

1. DATA TAKEN 9/5/81, 1 PM PDT
2. WEATHER: HAZY @ 76°F
3. 9.43 AMP. HOURS, 12:00 - 1:00 PM

Figure 33. High-Sun Nominal System Voltages and Currents

equipment on DC (solar) power, and some equipment on inverter (solar) power, all at the same time with no ill-effects. Checks with local stations and with stations located in Australia have indicated no noticeable hum. However, the DC-to-DC converter does cause a problem worth mentioning.

B. VOLTAGE DROPS

Although #4 weld cable was used between the battery box and the radio room, the 50-ft distance results in 100 ft of cable that has a measured DC resistance of 0.053 ohms each way (0.11 ohms round trip). This causes an impedance problem when the DC-to-DC converter is on. This power conditioner, which is located in the radio room, is used to produce the heater current for the final amplifier tubes and the plate voltage for the low-band transceiver when operating in the pure DC mode (inverter off). The converter produces a 100-Hz square wave, which gets rectified and filtered within the transceiver but which also can be seen and heard on the 12-V #4 weld cable line. Any other equipment such as the high-frequency radio connected to this line will see this pulse train. Therefore, a noticeable hum exists in the audio of the high-frequency radio. The problem was partially eliminated by putting 86,000 microfarads of capacity across the 12-V line which, at 100 Hz, effectively produces a capacitive reactance of 0.019 ohms. The capacitors are automatically removed from the 12-V line when the equipment is operated with the inverter or utility power.

C. RADIO ROOM CONTROL

Figures 34 and 35 show the inverter control, emergency lighting control, and radio room systems voltage monitoring.

The inverter is actuated by the closing of a 200-A hermetically sealed control relay that can be actuated from the battery box or the radio room. Placing +12 V on terminal 30 (Figure 34) actuates relay K1. Contact K1 closes, connecting 12 V to the input of the inverter. Since the input current to the inverter could be as much as 50 A, it is necessary to have a contactor that can switch that much current. The contactor is in a potentially rich hydrogen environment; therefore, it is important to have a hermetically sealed switching device. In any case, all switching devices that are electromechanical should be kept below the upper surface of the battery pack.

When the inverter is actuated from the radio room, a red light emitting diode indicates the ON state.

The inverter input and output are floating, as supplied by the manufacturer. In this system the inverter chassis, -12 V return, and 117 V AC low are made common so mixed modes of utility DC, inverter DC, and battery DC operation can safely be used.

Radio room lighting is controlled by manually actuating a switch on the control box (Figure 35). A voltmeter can be monitored by the operator. This meter measures the system DC voltage at the radio room. The operator must manually shut the system down when the system voltage drops below 11.3 V at the radio room.

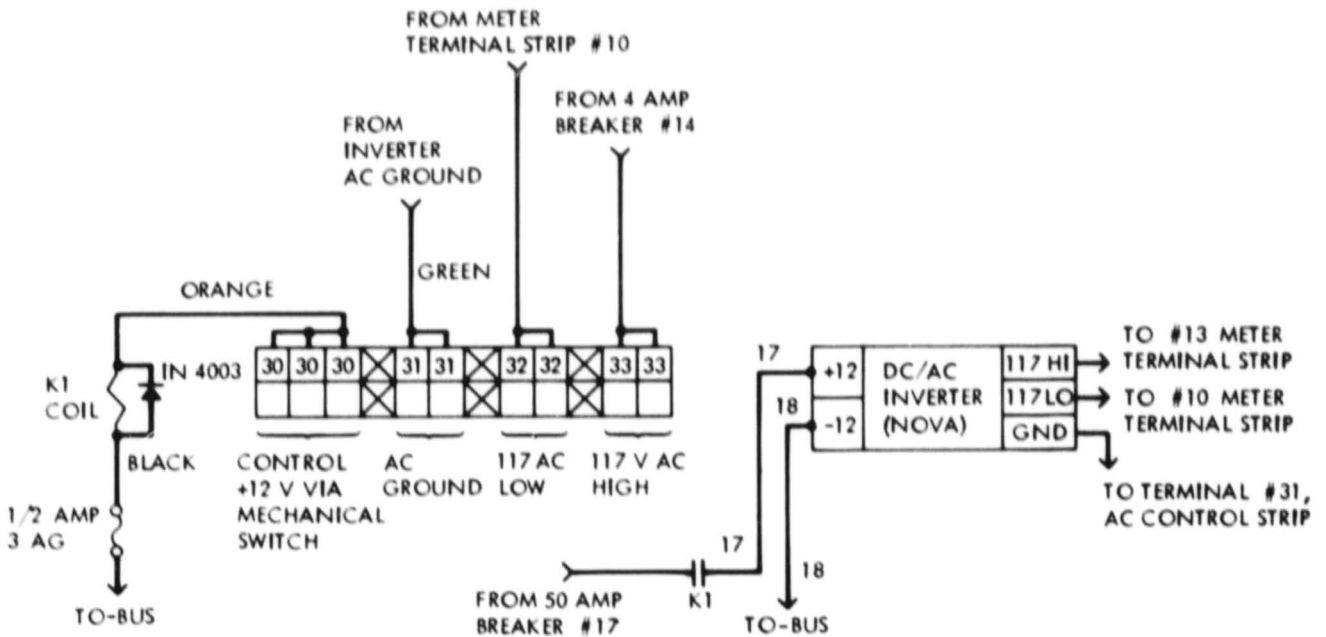


Figure 34. AC Control and Distribution Schematic Diagram

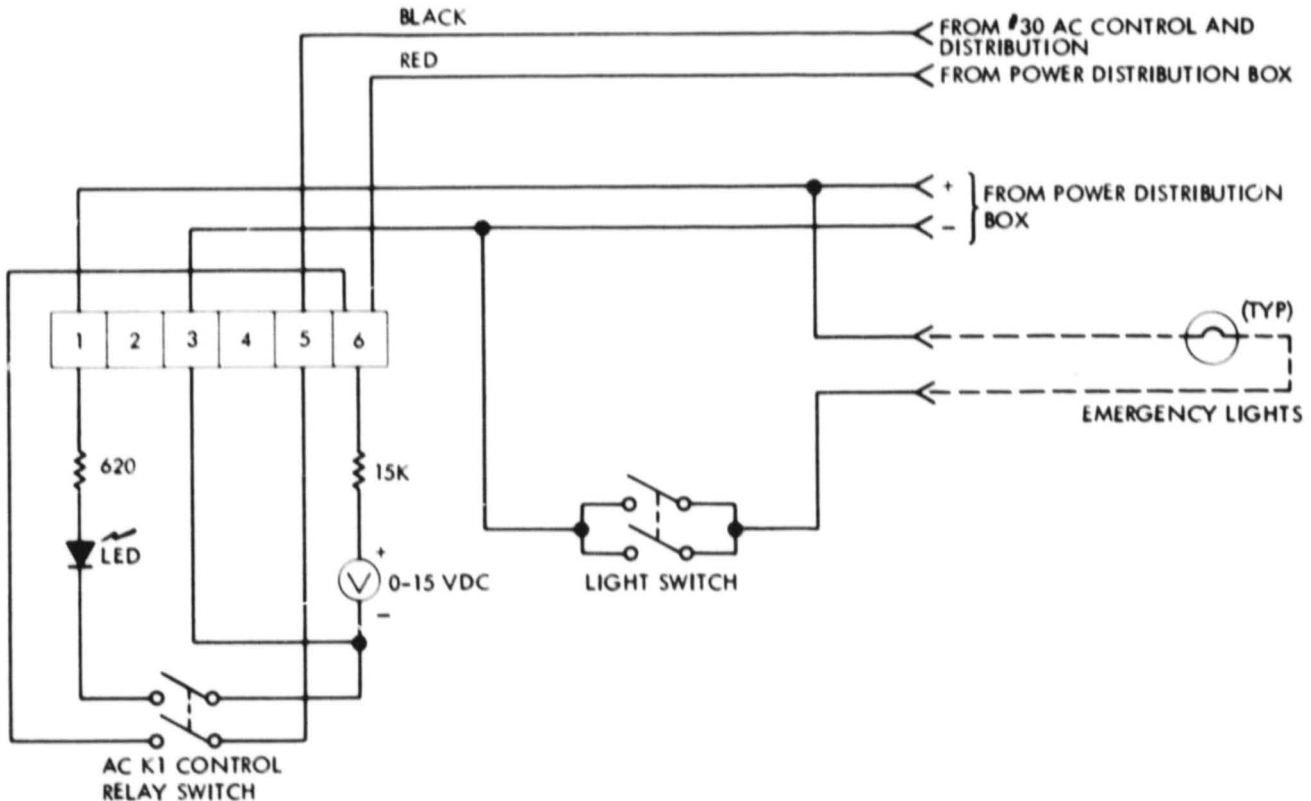


Figure 35. Radio Room Metering and Control Schematic Diagram

Table 10 indicates the steady-state DC current requirements for the equipment and the inverter. As can be seen in this table, it is more energy efficient to operate the low-band equipment in the DC mode rather than in the AC (inverter) mode, but higher output power can be achieved in the AC mode. The high-band equipment is normally operated in the DC mode.

D. SAFETY

A breaker box is provided for safety. Figure 36 shows the function of the seven aircraft-type breaker switches. Although 12-V systems appear to be relatively safe from shock hazard, a watch band, ring, or wrench between +12 and -12 V can be quite painful. All equipment is fused and all inverter AC distribution is wired to code with a third-wire ground carried through to all AC outlets. Finally, the array framework is grounded and all antennas can be disconnected from the equipment during electrical storms.

Table 10. Station Steady-State Current Overhead (Accumulative)

BAND	MODE	dc BATTERY CURRENT REQUIREMENTS	
		INVERTER (117 vac)	12 VOLTS dc
LOW	INVERTER ON	3.1 AMPS	-
	RECEIVE ONLY	6.2	1.2 AMPS
	FINAL HEATERS	8.1	4.8
	READY TO TRANSMIT**	10.0	7.7
HIGH	RECEIVE ONLY	-	0.1 AMPS
	TRANSMIT CARRIER - 10 WATTS*	-	1.4
	TRANSMIT CARRIER - 40 WATTS*	-	4.7

**NO SIDEBAND MODULATION OR CW CARRIER

*FM CARRIER ONLY - NO MODULATION

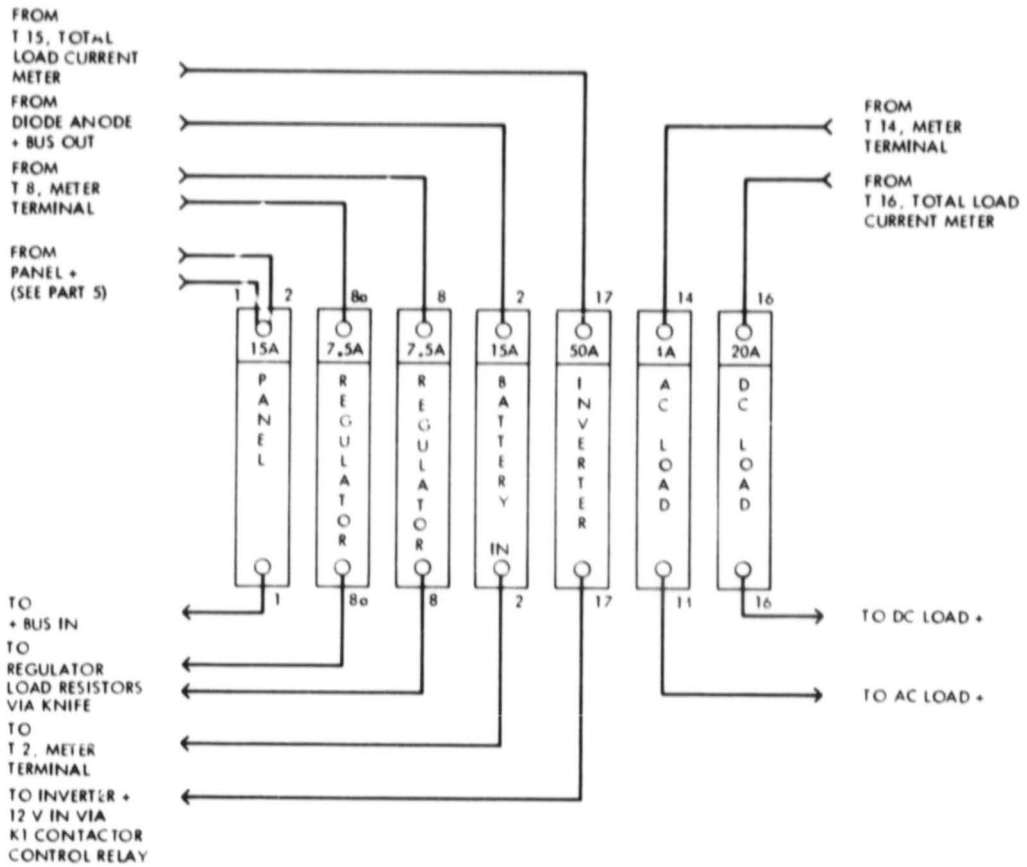


Figure 36. PV System Circuit Breakers

SECTION VI

SUMMARY, PHILOSOPHY, AND RECOMMENDATIONS

This report describes a low-power photovoltaic system in enough detail to allow similar systems (scaled up or down) to be constructed using the methodology developed, in part, from other engineering disciplines.

It is easy, in retrospect, to look back and see where the major time and effort were spent. The surprises centered around paper designs of PV system shunt regulators that could have never worked properly if built. In addition, it is amazing how inefficient low-voltage (12-V) inverters are. Techniques and new semiconductor devices are available to improve this poor performance. Much of the available commercial communications equipment is designed around 12 V DC and 117 V AC, so 12-V sine wave or pseudo sine wave inverters are desirable for these systems.

Much emphasis has been placed on increasing the efficiency of solar cells. Perhaps equally important areas of improvement are in battery development and complete characterization of these batteries for PV energy storage use. Battery temperature coefficients, Peukert constants, and constant power discharge coefficients are required to design cost-effective energy storage PV systems.

The PV manufacturers should present their I-V curves in increments of -10 mW/cm^2 from 100 or 80 mW/cm^2 and indicate that the curves translate linearly along the ordinate axis with irradiance. A few days of using a radiometer will convince most of us that a 100- mW/cm^2 day happens only occasionally--at least in and near metropolitan areas. An 80- mW/cm^2 day is perhaps more realistic.

Since there is an abundance of 12-V communications equipment being manufactured, it would be helpful if the PV module manufacturers would provide modules specifically designed for 12-V energy storage systems. This would assume 14.1-V float voltages, shunt-type regulators, and two diode drops. The system could then be operated at an optimum point on the I-V curves, unlike this system.

The system described herein has no moving mechanical parts except for a single relay and some analog meters. It is definitely impressive to sit at the radio room console and talk to someone across town or halfway around the planet, using a no-noise, nonrotating, nonpolluting energy source. We think that small systems as described here will appear in greater numbers as the cost of photovoltaics and inverters becomes more realistic. At present, however, the cost of these two important elements is restricting the construction of these types of low-power systems.

REFERENCES

1. Smokler, M. I., User Handbook for Block III Silicon Solar Cell Modules, DOE/JPL-1012-79/6 (JPL Internal Document 5101-82), Jet Propulsion Laboratory, Pasadena, Calif., February 1979.
2. Solar Cell Array Design Handbook, Volume 1, JPL SP 43-38, Jet Propulsion Laboratory, Pasadena, Calif., October 1976.
3. Revised Terrestrial Photovoltaic Measurement Procedures, NASA TM 73702, NASA Lewis Research Center, June 1977.
4. Ross, R. G., and Gonzales, C. C., "Reference Conditions for Reporting Terrestrial Photovoltaic Performance," Proceedings of the AS/ISES 1980 Annual Meeting, Phoenix, Arizona, June 1980.
5. TRW Power Semiconductors' 1980 Data Book, TRW, Lawndale, Calif.
6. Chapman, C. P., Fourier Transform Battery State of Charge Concepts, JPL Internal Document 5030-314, Jet Propulsion Laboratory, Pasadena, Calif., March 1979.
7. Cannone, A. G., Feder, D. O., and Biagetti, R. V., "Positive Grid Design Principles," The Bell System Technical Journal, pp. 1279-1303, September 1970.
8. Peukert, W., "On the Dependence of the Capacity of Lead-Accumulators on the Discharge Current," Elektro-Technische Z., (ETZ), 18, pp. 287-288, 1897.
9. Chapman, P., "Performance Characteristics of an Electric Vehicle Lead-Acid Battery Pack at Elevated Temperature," Jet Propulsion Laboratory, Pasadena, Calif. (Unpublished), July 1981.
10. Brennan, J., et al., Electric and Hybrid Vehicle Performance and Design Goal Determination Study, SAN/1215-1, Department of Energy (General Research Corporation CR-1-734), August 1977.
11. Chapman, P., "A Generic Battery Model for Electric and Hybrid Vehicle Simulation Performance Prediction," Electric Vehicle Council Expo, EVC Paper No. 8051, May 1980.
12. Klein, I. S., "Determining the Heat Generated in Advanced Lead-Acid Batteries for Electric Vehicles," Electrochemical Society Extended Abstracts, Volume 80-1, p. 24, May 11-16, 1980.
13. Yoder, C. M., and Schrag, M. L., "Nassi-Shneiderman Charts--An Alternative to Flowcharts for Design" Software Design Techniques--Third Edition, IEEE Catalog No. EHO 161-0, pp. 386-393, 1980.

14. Handbook for Battery Energy in Photovoltaic Power Systems, SAND 89-702Z, Bechtel National Inc., Final Report, pp. 2-5, 2-6, 3-23, 3-24, 3-25, November 1979.

APPENDIX

PROCEDURES FOR CALCULATING
THE AVERAGE TRANSMITTANCE OF SOLAR
ENERGY THROUGH THE EARTH'S ATMOSPHERE

APPENDIX

PROCEDURES FOR CALCULATING THE AVERAGE TRANSMITTANCE OF SOLAR ENERGY THROUGH THE EARTH'S ATMOSPHERE⁴

A. GENERAL

The solar constant at the top of the atmosphere is 135.3 mW/cm^2 . For perfectly clear atmosphere, assuming no terrain reflections or atmospheric diffusion, only the beam component of solar radiation will reach the collector, although the perfectly clear atmosphere will attenuate the radiation to something less than 135.3 mW/cm^2 . Hazy skies will attenuate the radiation even more as well as diffuse the radiation. Therefore, an average transmittance of the solar energy under hazy skies can be described, rather than just the attenuation of the beam component of the radiation through clear skies. The algorithms described in this Appendix will provide an estimate of the amount of solar radiation falling on a photovoltaic array given the site latitude, in degrees; the solar declination angle, in degrees; and the solar hour angle, in degrees. The precise value of declination varies from year to year since each year is 365.25 days long. The American Ephemeris and Nautical Almanac published each year by the U.S. Government Printing Office contains the precise declination values, but the table included in this Appendix should be adequate for these estimates.

B. SOLAR ALTITUDE ANGLE

The solar altitude angle, α , is measured from the site horizontal plane upward to the center of the sun. The angle, however, is not a fundamental angle but related to the hour angle, latitude, and solar declination by:

$$\sin(\alpha) = \sin(L) \sin(\delta) + \cos(L) \cos(\delta) \cos(h) \quad (\text{A-1})$$

where

α = solar altitude angle, degrees

L = site latitude, degrees

δ = sun declination angle, degrees (see Table A-1)

h = hour angle, degrees

⁴The equations and summary solar ephemeris table contained in this Appendix have been adapted and modified from The McGraw-Hill Operation Update Series in Solar Heating and Cooling, Manual One, Principles of Solar Geometry and Optics, Jan F. Kreider Editorial Advisor, McGraw-Hill, 1978.

Site latitude can be obtained from a local map or atlas. Sun declination angle can be approximated from Table A-1. The solar hour angle is equal to 15° times the number of hours from local solar noon. Values east of due south (i.e., morning values) are positive; values west, negative. The numerical value of 15° per hour is based upon the nominal time (24 hours) required for the sun to move around the earth (360°) once.

For example, given local time of 9:00 a.m. at 40° north latitude, December 25, the solar altitude angle is given by Eq. (A-1) to two-place accuracy as:

$$\sin \alpha = \sin(40^\circ) \sin(-23.42^\circ) + \cos(40^\circ) \cos(-23.42^\circ) \cos(45^\circ)$$

Table A-1. Summary of Solar Ephemeris

Month Date	Sun Declination Angle, Degrees							
	1	5	9	13	17	21	25	29
JAN	-23.07	-22.70	-22.22	-21.62	-20.90	-20.08	-19.15	-18.13
FEB	-17.32	-16.17	-14.92	-13.62	-12.25	-10.83	- 9.38	-
MAR	- 7.88	- 6.35	- 4.80	- 3.23	- 1.65	- 0.08	+ 1.50	+ 3.07
APR	+ 4.23	+ 5.77	+ 7.28	+ 8.77	+10.20	+11.58	+12.93	+14.22
MAY	+14.83	+16.03	+17.15	+18.18	+19.15	+20.03	+20.82	+21.50
JUN	+21.95	+22.47	+22.87	+23.17	+23.37	+23.45	+23.42	+23.28
JUL	+23.17	+22.87	+22.47	+21.95	+21.35	+20.63	+19.83	+18.95
AUG	+18.23	+17.20	+16.10	+14.92	+13.68	+12.38	+11.03	+ 9.65
SEP	+ 8.58	+ 7.12	+ 5.62	+ 4.10	+ 2.57	+ 1.02	- 0.53	- 2.10
OCT	- 2.88	- 4.43	- 5.97	- 7.48	- 8.97	-10.42	-11.83	-13.20
NOV	-14.18	-15.45	-16.63	-17.75	-18.80	-19.75	-20.60	-21.35
DEC	-21.68	-22.27	-22.75	-23.10	-23.33	-23.43	-23.42	-23.28

or

$$\sin \alpha = (0.64)(-0.40) + (0.77)(0.92)(0.71)$$

so

$$\sin \alpha = 0.25$$

and

$$\alpha = \arcsin (0.25) = 14.30^\circ$$

That is, the sun will appear about 14.3° above the site horizontal plane at 9:00 a.m. local time on December 25, at 40° north latitude.

C. CLEAR SKIES MODEL

The average solar radiation (beam component) through the atmosphere at the site elevation (feet above sea level) can be approximated by the following equations:

$$\bar{i}_{\text{atm}} = 0.5 \left[e^{-0.65m(Z,\alpha)} + e^{-0.095m(Z,\alpha)} \right] \quad (\text{A-2})$$

where

α = solar altitude angle, degrees

m = air mass at an altitude Z feet above sea level

$$m(Z,\alpha) = m(0,\alpha) \frac{p}{p_0} \quad (\text{A-3})$$

where

$$p/p_0 = 1.0057e^{-3.8181 \times 10^{-5}Z} \quad (\text{A-4})$$

and

$$m(0,\alpha) = \left[1229 + (614 \sin \alpha)^2 \right]^{1/2} - 614 \sin \alpha \quad (\text{A-5})$$

here

p/p_o = fraction of standard atmosphere at site elevation Z feet above sea level

For example, assume the solar altitude angle α at 12:30 p.m. on June 25 at a site was 76.7060° . Assume the site is 1,000 ft above sea level. The average transmittance is calculated in the following steps:

(1) from Eq. (A-5):

$$\begin{aligned}m(0,\alpha) &= \left[1229 + (614 \sin 76.7060)^2 \right]^{1/2} - 614 \sin 76.7060 \\ &= 598.57 - 597.55 \\ &= 1.02\end{aligned}$$

(2) from Eq. (A-4):

$$\begin{aligned}p/p_o &= 1.0057e^{-3.8181 \times 10^{-5} \times 1,000} \\ &= 0.97\end{aligned}$$

(3) from Eq. (A-3):

$$\begin{aligned}m(Z,\alpha) &= (1.02)(0.97) \\ &= 0.99\end{aligned}$$

(4) from Eq. (A-2):

$$\begin{aligned}\bar{\tau}_{atm} &= 0.5 \left[e^{-0.65(0.99)} + e^{-0.095(0.99)} \right] \\ &= 0.72\end{aligned}$$

That is, the beam component of the radiation at the top of the atmosphere must be multiplied by the $\bar{\tau}_{atm}$ factor:

$$\begin{aligned}I_b &= (0.72) (135.3 \text{ mW/cm}^2) \text{ beam component at site} \\ &= 97.42 \text{ mW/cm}^2\end{aligned}$$

Therefore, 97.42 mW/cm^2 is available for collection by the PV system according to this model. This can then be related back to the PV module I-V curves and SOC efficiency factor to predict array performance at 12:30 p.m. on June 25,

assuming the array is facing directly at the sun. If the above calculations are carried out to more than two decimal point places, a more exact figure of 96.99 mW/cm² will result.

D. HAZY SKIES MODEL

The average transmittance of solar energy through the atmosphere can be predicted for two levels of haze: 23-km (14-mi) haze and 5-km (3-mi) haze.

$$\bar{\tau}_{\text{atm}} = A_0 + A_1 e^{-k \text{ CSC}(\alpha)} \quad (\text{A-6})$$

where, for 23-km haze:

$$A_0 = 0.12755 + 0.10120(A) - 0.00964(A)^2 \quad (\text{A-7})$$

$$A_1 = 0.75686 - 0.07805(A) + 0.0064(A)^2 \quad (\text{A-8})$$

$$k = 0.38673 - 0.09047(A) + 0.01724(A)^2 \quad (\text{A-9})$$

and

α = solar altitude angle, degrees

and

A = site elevation in miles above sea level.

For 5-km haze at altitude A miles,

$$A_0 = 0.0270 + 0.07526(A) - 0.00611(A)^2 \quad (\text{A-10})$$

$$A_1 = 0.81015 + 0.01321(A) + 0.00109(A)^2 \quad (\text{A-11})$$

$$k = 0.75524 - 0.40500(A) + 0.08099(A)^2 \quad (\text{A-12})$$

also, $\text{CSC}(\alpha) = 1/\sin(\alpha)$.

For example, assume a solar altitude angle of 60° at solar noon at a site located 2,000 ft above sea level (0.38 mi above sea level). Assume a mildly hazy day which approximates a visibility of about 14 mi (23-km haze model). The average transmittance can be approximated by the following steps:

(1) from Eq. (A-9):

$$k = 0.38673 - 0.09047(0.38) + 0.01724(0.38)^2$$

$$k = 0.35$$

(2) from Eq. (A-8):

$$A_1 = 0.75686 - 0.07805(0.38) + 0.0064(0.38)^2$$

$$A_1 = 0.73$$

(3) from Eq. (A-7):

$$A_0 = 0.12755 + 0.10120(0.38) - 0.00964(0.38)^2$$

$$A_0 = 0.16$$

(4) $\sin(\alpha) = \sin(60^\circ) = 0.87$

$$\text{CSC}(\alpha) = 1/0.87 = 1.15$$

(5) from Eq. (A-6):

$$\bar{\tau}_{\text{atm}} = 0.16 + 0.73e^{-0.35(1.15)}$$

$$\bar{\tau}_{\text{atm}} = 0.65$$

If the solar radiation is 135.3 mW/cm^2 at the top of the atmosphere, only 135.3×0.65 or 87.95 mW/cm^2 will be available for collection by the PV array, on the average, since the haze attenuates and scatters the radiation before being intercepted by the array, according to this model. This can be related back to the module I-V curves and SOC efficiency to predict the array performance at the site, assuming a south-facing array generally facing the sun.